Price formation without fuel costs:
the interaction of demand elasticity with storage bidding

Tom Brown[a,*], Fabian Neumann[a], Iegor Riepin[a]

[a]*Department of Digital Transformation in Energy Systems, Institute of Energy Technology,*
Technische Universität Berlin, Fakultät III, Einsteinufer 25 (TA 8), 10587 Berlin, Germany

Abstract

Studies looking at electricity market designs for very high shares of wind and solar often conclude that the energy-only market will break down. Without fuel costs, it is said that there is nothing to set prices. Symptoms of breakdown include long phases of zero prices, scarcity prices too high to be politically acceptable, prices that collapse under small perturbations of capacities from the long-term equilibrium, cost recovery that is impossible due to low market values, high variability of revenue between different weather years, and difficulty operating long-term storage with limited foresight. We argue that all these problems are an artefact of modelling with perfectly inelastic demand. If short-term elasticity to reflect today's flexible demand (-5%) is implemented in the model, these problems are significantly reduced. The combined interaction of demand willingness to pay and storage opportunity costs is enough to produce stable pricing. This behavior is illustrated by a model with wind, solar, batteries, and hydrogen-based storage, where the price duration curve is significantly smoothed with a piecewise linear demand curve. This removes high price peaks, reduces the fraction of zero-price hours from 90% to around 30%, and guarantees more price stability for perturbations of capacity and different weather years. Fuels derived from green hydrogen take over the role of fossil fuels as the backup of final resort. Furthermore, we show that with demand elasticity, the long-term optimisation model exactly reproduces the prices of the short-term model with the same capacities. We then use insights from the long-term model to derive simple bidding strategies for storage so that we can also run the short-term model with limited operational foresight. We demonstrate this short-term operation in a model optimised using 35 years of weather data and then tested on another 35 years of unseen data. We conclude that the energy-only market can still play a key role in coordinating dispatch and investment in the future.

Keywords: electricity markets, price formation, capacity expansion, variable renewables, demand elasticity, storage bidding, energy-only market

JEL: Q400, Q410, Q420, C610, D410, D470

1. Introduction

1.1. Problem statement

In electricity markets dominated by fossil fuel generators, prices are set in most hours by the variable costs of the power plant on the margin. In hours of scarcity, when all generation is at full capacity, prices are determined by the demand's willingness to pay.

As more zero-marginal-cost generation from wind and solar enters the market, the supply curve shifts to the right, which reduces the market price, sometimes to zero or even negative values [1]. This so-called *merit order effect* puts pressure on the revenues of conventional generators as well as on variable renewables. If conventional generators leave the market, scarcity pricing could become more pervasive.

There is a widespread concern in the literature that if shares of wind and solar rise even higher, providing more than 80% of yearly electricity, prices might become so singular that the energy-only market might no longer function in a meaningful way [2]. Taylor et al. [3] express the concern 'because there are no fuel costs, employing nodal pricing as is would simply result in all prices being equal to zero'. Some simulations indicate that prices are not always zero, but zero most of the time, with very high prices in other hours. Mallapragada et al. [4] find that in 'VRE-dominant energy-only wholesale power markets . . . generators and storage facilities would earn the bulk of their annual energy market revenues in relatively few hours'. Similarly, Levin et al. [5] raise the concern that '. . . a large fraction of the value of [energy storage] may be realised during a relatively small number of periods'. A study for the Royal Society [6] suggests that 'if paid only on the basis of short-run costs, the large-scale long-term storage . . . could never recover its capital costs' and that 'traditional spot markets, which were developed to deal with gas and coal powered generation, are not automatically . . . adaptable to . . . wind, solar, and storage.'

Additional concerns include an expectation of wide swings in prices between different years reflecting changing weather conditions [7–9], raising risks around cost recovery [10–13], and concerns about how storage dispatch and prices behave when transitioning from long-term capacity expansion models with perfect foresight to short-term operational models with myopic foresight [14, 15]. The apparent challenge to secure sufficient revenue for assets needed for system reliability [16] has led to discussions about alternative market designs oriented towards capacity rather than energy provision [2, 17–19].

1.2. Other literature

Other modelling studies incorporating newly-electrified sectors and demand flexibility in systems with high renewable

---
[*]Corresponding author
Email address: t.brown@tu-berlin.de (Tom Brown)

shares have seen different behavior [20–23]. These studies see more moderate price duration curves with fewer zero and scarcity prices in capacity expansion models that incorporated flexible demands from heating, transport, and coupling to hydrogen production, which frequently becomes price-setting. Similar effects have been observed for systems with storage [24]. Even without the dominance of renewables, it has been noted that a small amount of demand elasticity can improve market operation, screening away price spikes [25–27]. Others point out that systems without fuel costs might not undermine the working principles of energy-only markets if taking into account storage operation, scarcity prices and demand response [28].

In power systems dominated by hydroelectricity, which also has near-zero marginal costs, it has been understood for decades how the opportunity costs for dispatch give the storage medium water a value [29–36], thereby determining the bidding behavior of hydroelectric generators. These insights have been recently transferred to the dispatch of long-duration energy storage (like hydrogen storage or thermal energy storage in district heating), where marginal storage values have been used in operational dispatch settings to develop bidding rules [37] and deal with myopic foresight [38]. Bidding strategies for storage have also been investigated by Ward et al. [39, 40] without optimisation methods, looking at how price variability affects the arbitrage earnings of storage.

A series of papers [41, 42] examines the price structure in a stylised setup with renewables and storage only and find that prices set by storage play an important role in the cost recovery of all assets. However, the analysis is simplified to a residual load duration curve setup without addressing intertemporal storage dynamics or storage capacity constraints. Furthermore, the authors assume perfectly inelastic demand and only one type of renewable generation and storage technology.

Antweiler and Müsgens [43] explore price formation and market equilibria using analytical and empirical models with wind, solar, and storage technologies and demand response. The authors show that energy-only markets remain functional even when the system only includes generators with near-zero marginal costs, as long as free entry and competition ensure effective price setting. However, the analysis is limited to a stochastic state space covering only one hour, so that the intertemporal dynamics of storage operation is not modeled explicitly.

Ekholm and Virasjoki [44] analyse pricing mechanisms in fully renewable systems with demand elasticity (-25%) under perfect and Cournot-type imperfect competition and identify the key role of storage operation and demand elasticity for price setting. They consider a short-term operational setting with weekly time frames without capacity expansion, multi-decadal time series, or myopic foresight.

De Jonghe et al. [45] describe different approaches to incorporate demand elasticity into capacity expansion models with perfect foresight, including cross-price elasticities between different hours. In a model with high conventional capacity and no storage, they find that demand elasticity increases the share of wind and reduces peak capacity required as demand response clears the market in those peak hours. However, their analysis does not focus on the price formation mechanisms.

Adachi et al. [46] include price-responsive demand in a model with renewables and storage, and find that 'stable average prices can be maintained throughout the transition to 100% VRE'. However, they did not consider multiple weather years, long-duration energy storage, or analyse the resulting price duration curves.

1.3. Main thesis

In this paper, we provide analytic insights and modelling results to provide a unifying framework for understanding price formation at high penetrations of variable renewables like wind and solar. We show how storage bidding and demand flexibility combine to stabilise price formation. We use a model complex enough to illustrate the salient points, yet simple enough to trace cause and effect.

Our novelty lies in comparing price formation in systems with high shares of variable zero-marginal cost generation under different demand modelling paradigms, various levels of operational foresight, and across an order of magnitude more weather conditions than used previously in the literature. This allows us to disentangle the contradictory results from the literature and explain them as particular corners of the solution space. In addition, we use state-of-the-art recent measurements of demand elasticity [47, 48] to enhance the realism of our simulations.

Our main contention is that much of the singular price behavior observed in the literature stems from the assumption of perfectly inelastic demand used in capacity expansion models for electricity. If more realistic demand behavior is used, with, for example, the -5% short-term price elasticity of demand at the average price that was recently observed from today's industrial consumers in Germany [47, 48], then many artefacts resulting from assuming perfectly inelastic demand disappear. Prices no longer jump between zero and scarcity; they remain stable over many weather years and do not collapse with small capacity perturbations. This explains the smoother price results observed in sector-coupling studies that include demand flexibility (although this is often modelled with virtual storage units rather than explicit demand curves) [20, 21, 23]. Furthermore, demand elasticity also smooths the marginal storage values for long-duration energy storage, which allows us to deduce heuristics for storage bidding based on these marginal values and dispatch the systems with myopic foresight similar to [38].

In addition to developing an understanding of these features theoretically through the interaction of shadow prices in the optimisation model, we also provide hourly modelling simulations for three European countries featuring different renewable potentials (Germany, Spain, and the United Kingdom) with over 70 years of weather data. The present study is the first study we are aware of that considers demand elasticity in such capacity expansion models with multi-decadal time series. Solving such models is enabled by innovations in interior-point solvers for such convex problems [49]. We illustrate price formation for various demand types and examine which demand modelling approaches cause the price formation mechanisms to diverge or align between long-term models with capacity expansion and short-term models with only dispatch variables. We then show how prices behave under capacity perturbations from the long-term equilibrium, how well simple storage bidding heuristics can reproduce the price formation with realistic myopic operational foresight, and how this affects cost recovery.
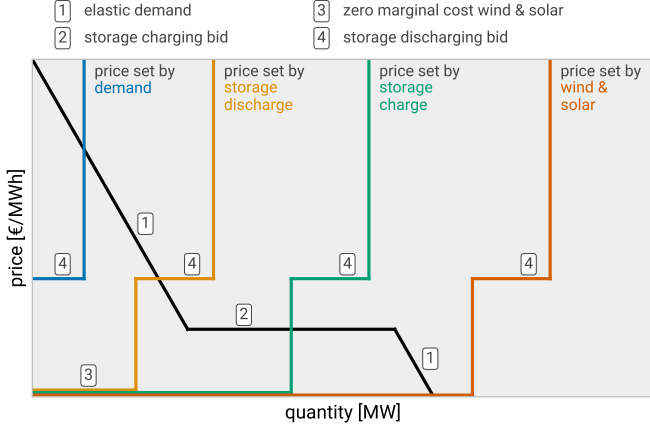
Figure 1: Example market situations with demand curve ((1) and (2)) and supply curves ((3) and (4)) for four different VRE feed-in situations. Depending on the VRE availability, either the demand (1), storage (2) and (4) or wind and solar production (3) sets the price.

2. Theory

2.1. Introduction

We first provide some intuition by examining hourly supply and demand curves for a system with zero-marginal-cost variable renewable energy (VRE), a single infinite[1] storage technology and demand elasticity. Fig. 1 shows how the price setting works with rising availability of VRE.

In the aggregated demand curve, part of the demand curve (1) is determined by the regular electricity demand, which is assumed to have elasticity with a low magnitude (e.g. below -5% at the average price). The other part is the willingness to pay for the storage charging (2). The storage willingness to pay is non-zero because the storage medium has a value. For hydrogen storage, this would correspond to the option to sell the hydrogen for a non-zero price.

The supply curve has two price levels: zero for VRE (3) and non-zero for the storage discharging (4). The storage bids with a non-zero price into the market because there is always an opportunity cost of saving energy to dispatch later in higher-price hours. This translates to a marginal storage value (MSV) of the storage medium. This MSV is also called the *water value* or *Bellman value* in the water resource management and hydroelectricity literature [30–32]. For a storage medium like hydrogen, it would correspond to the market price of the hydrogen.

As a result of these bidding curves, the electricity price is only zero in the case that the VRE availability exceeds both the peak of the regular demand and the storage charging capacity. When demand exceeds VRE feed-in but not the available storage discharging capacity, then storage discharging sets the price based on the MSV. When VRE feed-in exceeds demand but not the storage charging capacity, then storage charging is price-setting. Finally, when demand exceeds VRE and storage, prices are set by the willingness to pay for the regular demand, resulting in some scarcity pricing.

This scarcity pricing is important because it helps to set the opportunity costs of the storage, which can hold back energy for

---

[1]Scarcity and cost in energy storage capacity would introduce multiple price levels for charging and discharging bids over time (Fig. S2).

these high-priced hours. Because the demand curve is sloped, the storage constantly makes trade-offs for how long to hold its energy, store it, or discharge it. The opportunity costs set the MSV, which in turn determines the electricity prices in most hours through the storage bidding.

2.2. Mathematical theory

This section provides a mathematical representation of the price formation by mapping the prices to dual variables (or *shadow prices*) of an optimisation problem. We first start with the long-term (LT) capacity expansion problem, in which the capacities of all assets are co-optimised with their dispatch. In the next section we look at the consequences of moving to a short-term (ST) model, where we fix all the capacities and optimise only the dispatch.

The long-run welfare maximisation runs over electricity consumers c, generators r, and storage units s, each of which can have different costs and efficiencies. The yearly welfare is represented by hourly weather and load conditions t. The optimisation variables are the dispatch for each period t of demand $d_{c,t}$, generation $g_{r,t}$, storage discharging $f_{s,t}$, charging $h_{s,t}$ and state of charge $e_{s,t}$ as well as capacities for each generator G_r, storage discharge F_s, charging H_s and energy E_s.

$$\max_{d_{c,t},g_{r,t},G_r,f_{s,t},F_s,h_{s,t},H_s,e_{s,t},E_s} \left[\sum_{c,t} U_{c,t}(d_{c,t}) - \sum_r c_r G_r - \sum_{r,t} o_r g_{r,t} \right.$$
$$\left. - \sum_s \left(c_s^f F_s + c_s^h H_s + c_s^e E_s \right) \right] \quad (1)$$

Specific annual fixed costs c_*, made up of annualised investment costs and fixed operation and maintenance costs, are applied for all assets, while linearised variable costs o_r are given only for generators. We assume non-linear utility for the demand and linear bidding for generation, assuming constant short-term marginal generation costs.

The constraints are split into hourly energy conservation for electricity and each storage medium s, and capacity constraints:

$$\sum_c d_{c,t} + \sum_s h_{s,t} - \sum_r g_{r,t} - \sum_s f_{s,t} = 0 \quad \leftrightarrow \quad \lambda_t \in \mathbb{R}$$
$$e_{s,t} - e_{s,t-1} - \eta_s^h h_{s,t} + (\eta_s^f)^{-1} f_{s,t} = 0 \quad \leftrightarrow \quad \lambda_t^s \in \mathbb{R}$$
$$-d_{c,t} \leq 0 \quad \leftrightarrow \quad \underline{\mu}_{c,t}^d \geq 0$$
$$d_{c,t} - D_{c,t} \leq 0 \quad \leftrightarrow \quad \bar{\mu}_{c,t}^d \geq 0$$
$$-g_{r,t} \leq 0 \quad \leftrightarrow \quad \underline{\mu}_{r,t}^g \geq 0$$
$$g_{r,t} - G_{r,t} G_r \leq 0 \quad \leftrightarrow \quad \bar{\mu}_{r,t}^g \geq 0$$
$$-f_{s,t} \leq 0 \quad \leftrightarrow \quad \underline{\mu}_{s,t}^f \geq 0$$
$$f_{s,t} - F_s \leq 0 \quad \leftrightarrow \quad \bar{\mu}_{s,t}^f \geq 0$$
$$-h_{s,t} \leq 0 \quad \leftrightarrow \quad \underline{\mu}_{s,t}^h \geq 0$$
$$h_{s,t} - H_s \leq 0 \quad \leftrightarrow \quad \bar{\mu}_{s,t}^h \geq 0$$
$$-e_{s,t} \leq 0 \quad \leftrightarrow \quad \underline{\mu}_{s,t}^e \geq 0$$
$$e_{s,t} - E_s \leq 0 \quad \leftrightarrow \quad \bar{\mu}_{s,t}^e \geq 0 \quad (2)$$

$D_{c,t}$ is the constant upper limit on the demand, while $G_{r,t}$ is the time-dependent availability factor for each generator. The electricity price corresponds to the shadow price of the energy

balance constraint λ_t, while the MSV for each storage unit is given by λ_t^s of the storage balance constraint.

The price formation can be deduced from the stationarity equations of the Karush-Kuhn-Tucker (KKT) conditions.[2] For the generation, we have

$$0 = \frac{\partial \mathcal{L}}{\partial g_{r,t}} = \lambda_t - o_r + \underline{\mu}_{r,t}^g - \bar{\mu}_{r,t}^g \quad \forall r, t. \tag{3}$$

The generator's variable cost o_r and available capacity determine its bid into the market. When a generator r is on the margin, so that neither capacity limit is binding, $\bar{\mu}_{r,t}^g = \underline{\mu}_{r,t}^g = 0$, the generator's variable cost is price-setting $\lambda_t = o_r$. This corresponds to part (3) of the supply curve in Fig. 1.

If we now consider the storage dispatch,

$$0 = \frac{\partial \mathcal{L}}{\partial f_{s,t}} = \lambda_t - (\eta_s^f)^{-1} \lambda_t^s + \underline{\mu}_{s,t}^f - \bar{\mu}_{s,t}^f \quad \forall s, t, \tag{4}$$

it has the same form as a generator bidding with variable cost $(\eta_s^f)^{-1} \lambda_t^s$, similar to a generator with a fuel cost of the value of the storage medium λ_t^s with conversion efficiency η_s^f. The term $(\eta_s^f)^{-1} \lambda_t^s$ corresponds to the *effective bid* of the storage dispatch variable $f_{s,t}$ obtained from Lagrangian relaxation [51]. If it is on the margin, it is price setting. We see here how the MSV λ_t^s sets the prices like fuel costs. This corresponds to part (4) of the supply curve in Fig. 1.

On the demand side, each demand satisfies

$$0 = \frac{\partial \mathcal{L}}{\partial d_{c,t}} = U_{c,t}'(d_{c,t}) - \lambda_t + \underline{\mu}_{c,t}^d - \bar{\mu}_{c,t}^d \quad \forall c, t, \tag{5}$$

where the derivative of the utility determines its demand curve. This corresponds to part (1) of the demand curve in Fig. 1, where the demand is price setting.

If we now consider the storage charging,

$$0 = \frac{\partial \mathcal{L}}{\partial h_{s,t}} = \eta_s^h \lambda_t^s - \lambda_t + \underline{\mu}_{s,t}^h - \bar{\mu}_{s,t}^h \quad \forall s, t, \tag{6}$$

it has the same form as a demand bidding with a willingness to pay $\eta_s^h \lambda_t^s$, i.e. it needs an electricity price low enough that it can sell storage medium at its going price λ_t^s considering its conversion efficiency η_s^h. This corresponds to part (2) of the demand curve in Fig. 1.

From this, we see how relevant the marginal storage values λ_t^s are in setting prices, since parts (2) and (4) both depend on them.

2.3. Conditions for matching prices in long-term and short-term models

In the long-term model (LT), storage and generation capacities are endogenous variables of the optimisation problem. In this case, fixed costs play a role in determining capacity investments that satisfy demand in a way that maximises social welfare. In the short-term model (ST), the capacities G_r, F_s, H_s, E_s are fixed from the beginning and not part of the optimisation.

It is not obvious that there is a relationship between the hourly prices in the LT and ST optimisation models. Economic theory suggests they should converge, since if the ST model deviates from the LT equilibrium, asset owners should notice that they are making either losses or excess profits and then (in the long-term) exit or enter the market respectively. However, from the perspective of the optimisation models, they have different sets of variables and objective functions. The ST model doesn't see the fixed costs of the assets at all, and the ST objective function only involves dispatch variables:

$$\max_{d_{c,t}, g_{r,t}, f_{s,t}, h_{s,t}, e_{s,t}} \left[\sum_{c,t} U_{c,t}(d_{c,t}) - \sum_{r,t} o_r g_{r,t} \right]. \tag{7}$$

If all variable costs are zero ($o_r = 0$), only the demand utility has non-zero coefficients in the objective function.

By taking the optimal capacities G_r, F_s, H_s, E_s from the long-term model and fixing them as constants in the short-term model, we can compare the resulting electricity prices λ_t. Economic theory says the ST and LT should have the same prices, but we will show that in the optimisation models, this only occurs under certain conditions. As a result, prices from LT optimisation models should be treated with care.

The key point is that in the presence of storage the fixed costs from the LT objective, i.e. the terms multiplied with c_* in (1), can mix themselves into the prices. This causes price deviations versus the ST model, where these fixed cost terms are not present. Without storage, the fixed costs are usually screened away in the screening curve analysis by a combination of the variable costs of the generators o_* and the cost for load shedding in the form of the value of lost load (VOLL) [52]. With storage, the fixed costs for the storage play a critical role in setting the marginal storage values (MSV) λ_t^s, since the MSV enable the storage to recover their fixed costs from price arbitrage. The MSV then leach into the market prices whenever the storage is price setting.[3]

We will now demonstrate that, in the presence of storage, the LT and ST model prices are identical as long as the aggregated inverse demand curve (aggregate of $U_{c,t}'$) provides a unique mapping from the demand to the price through a strictly monotonically decreasing demand curve. If there are steps[4] in the shape of the demand curve, the prices in the LT and ST model can diverge.

Suppose that there are no constraints on $d_{c,t}$, so that $\underline{\mu}_{c,t}^d = \bar{\mu}_{c,t}^d = 0$ for all c and t. Furthermore, suppose that the generation and load conditions in each hour are different so that there is a unique long-term solution for the demands $d_{c,t}$, i.e. there are no degeneracies between hours in the objective, so that load cannot be moved from one hour to another without a cost impact.

It follows that the optimal demands $d_{c,t}$ and generation and storage dispatch in the LT model must be identical to those in the ST model. This is because generation capacities are the same in both models, and any improvement to the objective

---

[2]The KKT conditions are the first-order conditions necessary for an optimal solution. When the objective function to maximise is concave, and the constraints are affine, these conditions are also sufficient for optimality [50].

[3]On a mathematical level, the fixed costs interact with the prices via the $\bar{\mu}$ variables in equations (3)-(6), which are then linked to the fixed costs via the stationarity equations for the capacity variables in the LT optimisation problem, e.g. for storage energy capacity $0 = \frac{\partial \mathcal{L}}{\partial E_s} = -c_s^e + \sum_t \bar{\mu}_{s,t}^e$ [51].

[4]Steps would represent segments of perfectly elastic demand, e.g. load shedding for a fixed value of lost load (VOLL).

function by altering dispatch variables in one model would also benefit the other.

If there is a unique mapping from the demand curve to prices from stationarity for $d_{c,t}$ (cf. Eq. (5)), and the demand curves are identical, then it follows that the prices must also be identical in both models in all hours. In other words, if there is a smooth elastic demand curve with a different price for each demand, prices will be identical. This holds even for very low elasticity values.

However, if the demand curve is a step function, such as with a VOLL at 2000 €/MWh, then prices are only identical during load shedding or excess supply hours in the absence of other generators with non-zero marginal cost. In the hours with load shedding, prices reach 2000 €/MWh in both the ST and LT models. In hours with excess supply beyond the storage charging capacity, prices are zero in both models. The constant demand for varying prices during non-shedding periods causes a demand-side degeneracy, which means the supply-side sets the price unless storage charging does. As fixed costs can set the price in the LT model but not in the ST model, we no longer have identical prices.

Symmetrically, if the supply curve were strictly monotonically increasing, e.g., with a variety of generators with different efficiencies and fuel costs, rather than in linear steps, this would also be sufficient to resolve the prices and guarantee identical prices between ST and LT models. Some structure is needed either on the supply or the demand to eliminate the degeneracy of prices.

3. Methods for simulations

3.1. Implementation details

To demonstrate how price formation works, modelling is done for three European countries (Germany, Spain, and the United Kingdom) using 70 years of historical hourly weather data from 1951 to 2020 [53]. We use 70 years of data for different countries to capture a wide variety of weather conditions, rather than illustrating a 70-year pathway of system transformation. Systems are modeled with only a limited selection of technologies: onshore wind, utility-scale solar photovoltaics, batteries for short-term storage, and a hydrogen-based chemical storage medium for long-term storage (e.g. underground hydrogen storage). The techno-economic parameters, such as investment costs and efficiencies, are provided in Table S1. The figures in the main body show results for Germany, while the results for Spain and the United Kingdom are provided in Appendix F.

The modelling framework used is Python for Power System Analysis (PyPSA) [54], and the open source code to reproduce our experiments is available on GitHub;[5] output data were deposited on Zenodo.[6] The experiments were run on a high-performance computing cluster with PyPSA v0.27.1 [54], linopy v0.3.8 [55], and Gurobi v11.0.2 [49]. For the resulting linear (LP) and quadratic (QP) problems, we used the interior point method without crossover, a barrier convergence tolerance of 10^{-7}, and 32 threads per model. The maximum memory requirement per scenario was 22 GB.
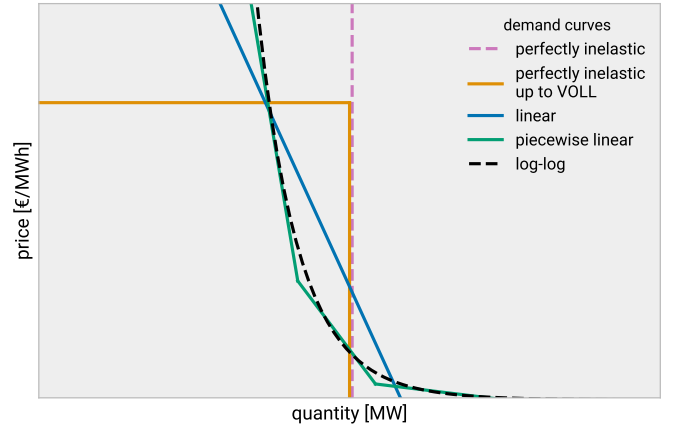

Figure 2: Illustration of different demand curves considered in the scenarios.

In this setup, we then vary the number of weather years in the simulation, the choice of the demand curve (Section 3.2), long-term optimisation with capacity expansion versus short-term optimisation with fixed capacities, capacity perturbations of ±5% around the long-term equilibrium, and myopic versus perfect foresight dispatch (Section 3.3).

3.2. Demand modelling

A single demand curve is modelled to represent all aggregated consumers. The demand curve is varied between a perfectly inelastic demand, an inelastic step function up to VOLL, a linear demand curve, and a piecewise-linear (PWL) approximation of a log-log demand curve, as shown in Fig. 2. For most of the modelling analysis we focus on the case of inelastic demand up to VOLL, since this is the common modelling approach and also reflects the price caps enforced in many markets, and the PWL log-log elasticity case, since this was empirically measured in the German market [48]. Non-linear curves are not considered because solving becomes inefficient once we go beyond quadratic terms in the objective function. The same demand curve is used for each hour to isolate effects of supply from demand. The level of demand is chosen to represent a token average of 100 MW in each country to simplify case comparisons.

The simplest case of perfectly inelastic demand is modelled by removing the utility from the objective function, since it is effectively infinite, and replacing the demand variable by a demand constant.

The next simplest case is that of demand that is completely inelastic up to a given value of lost load (VOLL). For a given demand $0 \leq d \leq D$ with value of lost load V, the utility function is

$$U(d) = Vd \tag{8}$$

The demand curve is a step function. It is perfectly inelastic up to a price of $p = U'(d) = V$, at which point it is perfectly elastic. Implementing this demand function in the optimisation problem Eqs. (1) and (2) results in a linear problem (LP). For the modelling we assume a VOLL of $V = 2000$ €/MWh and a peak load of $D = 100$ MW.

For a linear demand curve, the utility is quadratic:

$$U(d) = ad - \frac{b}{2}d^2 \tag{9}$$

giving a linear demand curve

$$p = U'(d) = a - bd \qquad (10)$$

This results in a quadratic problem (QP), similar to one of the approaches in De Jonghe et al. [45]. For a linear demand curve, the elasticity varies along it, becoming more elastic at higher prices. Using parameters $a = 2000$ and $b = 20$ results in an elasticity of -5% near the approximate average system price $p = 100$ €/MWh.

To approximate a demand curve of log-log form $\ln(p) = a - b\ln(d)$ with constant price elasticity, we use an aggregated demand curve given by several demands $d \in [0, D]$ with different constants (a, b), so that we get a piecewise-linear curve with different slopes. In Fig. 2, an example approximation is shown with three linear segments. Here, we use three segments with parameters $a = (8000, 400, 200)^\top$, $b = (80, 40, 20)^\top$, and $D = (95, 5, 10)^\top$, which results in an elasticity of -5% at a price of 100 €/MWh and a demand around 100 MW. The elasticity of -5% reflects the empirical analysis of the German market made in [48]. For sensitivity cases with higher and lower elasticity at the same price levels, coefficients a and b are halved or doubled which results in elasticities of -10% and -2.5% respectively at a price of 100 €/MWh.

In our main scenarios, we assume for simplicity that there are no inter-temporal dependencies for the demand elasticity, i.e. the demand level d_t at time t only depends on the price p_t. This is consistent with how the empirical measurements of German elasticity were made, since the inter-temporal effects were already present in the data [48]. In reality there may be complex dependencies on the hours before or after. In particular, some loads may not be able to reduce their demand for multiple consecutive hours, or they may have to increase the demand later to recover the lost demand. This can be represented in the model with cross-price elasticities between different hours [45], which adds bilinear terms between the hourly demands in the objective and does not affect our theoretical analysis, or by representing load shifts using a virtual storage for the demand, which is a common approach for e.g. flexible electric vehicle charging or heat pump operation [56]. In Appendix B, we show in a sensitivity analysis that cross-elastic terms have only a limited effect on our results.

To enhance numerical stability, we substitute demand variables with load-shedding generators as described in Appendix A, yielding identical results. Notably, the QPs with demand elasticity were observed to solve much faster than the LPs with perfectly inelastic demand up to the VOLL (6-16 times; 8-13 min vs. 72-144 min).

3.3. Myopic dispatch

Assuming perfect foresight over multiple years, where future periods of scarcity and abundance are fully anticipated, is unrealistic. While forecasts may be reliable 1-3 days ahead, and hydroelectric planners are accustomed to making seasonal forecasts for water levels in their dams, the multi-week time scales on which wind power vary are harder to anticipate in advance [57]. In particular this creates challenges for the dispatch of long-duration storage so that it charges during days of excess in order to discharge during periods of scarcity outside the myopic foresight horizon.

To evaluate the impact of myopic foresight on price formation for different demand modelling cases, we initially derive

optimised capacities from an LT model optimised using 35 randomly selected years from the 70-year dataset (Appendix D). Subsequently, we run the dispatch in an ST model using the remaining 35 years, comparing cases with perfect foresight with those with myopic foresight. We also apply perturbations of ±5% to all generation, conversion and storage capacities, to show the impacts of imperfectly anticipating the system's needs.

For cases with myopic foresight, we apply a rolling-horizon dispatch optimisation with a 96-hour look-ahead horizon and a 48-hour overlap between windows. This approach aligns with the horizon of current forecast skill and provides sufficient information for the short-term battery operation [57]. Since there are already good weather forecasts up to 5 days ahead [57, 58], this represents a conservative worst case for the system dispatcher.

For the chemical storage, we dispatch assuming a constant fuel value equal to the mean of λ_t^s from the LT model. For instance, if the hydrogen has an average value $\langle \lambda_t^s \rangle = 100$ €/MWh, the electrolysis with efficiency 70% bids 70 €/MWh for consuming electricity and the hydrogen turbine with efficiency 50% offers it at 200 €/MWh. By implementing these approximate bids as marginal costs on the storage, we use the average MSV as an orientation to operate long-term storage reasonably without foresight.[7]

However, although λ_t^s becomes relatively stable when demand elasticity is modeled (Fig. 3),[8] assuming a constant value is not perfect for short-run dispatch and will cause price deviations from perfect foresight, which are quantified in Section 4.5.

A similar methodology was employed in [38], utilising a state-of-charge-dependent storage value, as also noted in [24]. In contrast, we maintain a simpler method with a constant MSV to demonstrate that reasonable results can be achieved even with this simplification. This assumption could be justified if industrial offtake users with long-term contracts and producers on global markets contribute to stabilising the hydrogen price.

4. Results

4.1. Results from the long-term model

Fig. 3 shows different price duration curves from the model with perfectly inelastic demand up to a value of lost load (VOLL) of 2000 €/MWh (left column) and with a piecewise-linear (PWL) approximation of -5% price elasticity of demand (right column). The results assume hydrogen is used for long duration storage.

Panels a) and b) in Fig. 3 reveal how the electricity price duration curves from the long-term model vary as the number of years in the simulation is increased from one year up to the full 70 years (Appendix D). For a duration curve to be meaningful, it should not change significantly as the number of years increases, but for the perfectly inelastic case, it becomes more and more singular as more years are considered. This is because high prices are clustered into the wind-scarce years,

---

[7]Knowing the marginal storage value λ_t^s of the ST model in advance would be sufficient to reproduce the optimal dispatch with perfect foresight, as illustrated by the effective bids of Lagrangian relaxation [51].

[8]In order for the chemical storage itself to recover its capital costs from arbitrage, the marginal storage value λ_t^s has to vary. It would only be constant if the storage capacity were free and unconstrained (Fig. S2).
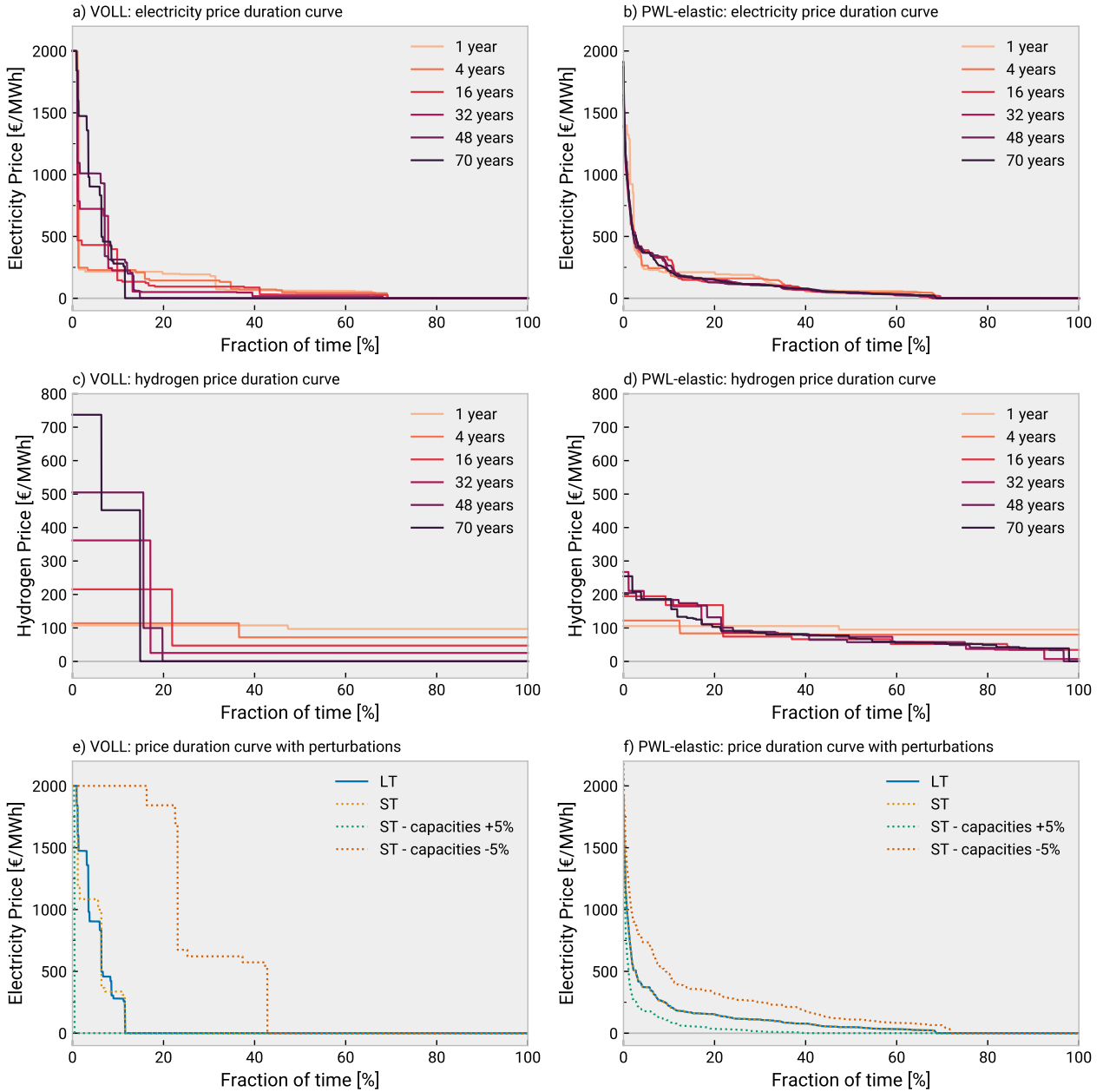
Figure 3: Different price duration curves: Panels a) and b) show electricity price duration curves as the number of years used in the optimisation rises from 1 to 70. Panels c) and d) show the corresponding hydrogen price duration curves for the same simulations. Panels e) and f) show for the 70-year optimisation how the prices change when going from the long-term (LT) to short-term (ST) model with the LT capacities, and then perturbing the asset capacities in the ST model up and down by 5%.

which drive the investment (Fig. S12). As the high prices cluster in the worst weather years, prices at other times collapse, since at these times there is over-capacity. For the case with demand elasticity, the elastic demand curve spreads the scarcity pricing out over the years, resulting in price duration curves that have a more consistent shape as the number of years in the model is varied. Furthermore, going from the perfectly inelastic to the price-responsive case for 70 years of data, the fraction of zero-price hours reduces from 89% to 31%, and the fraction of hours with prices over 400 €/MWh reduces from 8.5% to 3.9% so that the extreme variability of prices is substantially damped. This means that revenues for most technologies are more evenly distributed across different price bands (Fig. S9) instead of being concentrated in just a few high-priced hours. These results reproduce observations from sector-coupled models

[20, 23], where demand elasticity plays the same role as demand flexibility to reduce and stabilise prices.

We conclude from this that price duration curves from models with perfectly inelastic demand are not robust enough between simulations that anything can be deduced from them. Strong price bifurcations seen in previous studies (e.g. [4]) are modelling artefacts that cannot be taken at face value, since they are not consistent as the simulation length is changed and they depend strongly on how demand is modelled.

Panels c) and d) in Fig. 3 show hydrogen's corresponding price duration curves. Since hydrogen can be inexpensively stored in underground caverns (≈ 0.15 €/kWh, cf. Table S1), its price is more stable between different hours. This is because between periods of scarcity there is no system benefit in moving hydrogen between hours without binding capacity constraints.

However, it still shows variations between wind-scarce and windy years (Fig. S12). The price variability is much more extreme for the perfectly inelastic case, mirroring the tight coupling between electricity prices and marginal storage values.

Per unit of electricity supplied, the system cost in the elastic case is also 9.3% lower than in the inelastic case, as higher demand curtailment replaces some storage capacity (Table S4, Fig. S6). For the inelastic case, we observe 70 MW of firm capacity compared to 46 MW for the elastic case, which results in more regular demand curtailment over 70 years which, in effect, spreads the prices more evenly. In the inelastic case, there is less frequent load shedding concentrated in bad weather years that causes very high prices, while we trade this in the elastic case for more regular load reductions that cause much milder price increases.

4.2. Results from short-term model with perfect foresight

Panels e) and f) in Fig. 3 show the results of taking the optimal capacities from the long-term (LT) model, fixing them, and rerunning the operational short-term (ST) optimisation of the model with the same weather years and perfect operational foresight. We then perturb all capacities of generation and storage up and down by 5% to reveal how sensitive the prices are to capacities away from the long-term equilibrium.

Going from the LT to the ST model, we see the result of the theoretical argument in Section 2.3 confirmed: the prices are identical for demand elasticity, where we have a unique mapping from demand to price, but for the perfectly inelastic case the lack of price regularisation causes the prices of the ST model to diverge from the LT prices. Furthermore, prices are susceptible to small capacity perturbations, either becoming very high in many hours if capacity is tight or collapsing to zero if capacities are slightly over-dimensioned. In the elastic case, the price changes follow the same direction but are milder in magnitude and more regular over time. Average prices rise by 104% with 5% less capacity and go down by 63% with 5% more capacity (Table S4), incentivising market exits or entries with investments towards the long-term equilibrium.

4.3. Forcing dispatchable capacity to limit load reduction

Demand elasticity means that there are more regular reductions in demand, as can be seen from the load duration curves in Fig. S6. This can be a problem for some consumers if the reductions last more than a few hours. In our results there are reductions of 20% lasting 1-2 days roughly every other year during dark wind lulls, while there are 2 events in the 70 year sample lasting 10 days. To mitigate these high price events, we explore in Fig. S4 how forcing dispatchable capacity affects the model.

If some conventional dispatchable capacity is retained (Fig. S3) or power capacity for re-electrification of hydrogen is procured outside the energy-only market (Fig. S4), our results remain largely unchanged. Some high-price episodes gradually disappear, both for the inelastic and elastic cases, as scarcity costs of power deficits are replaced by the cost of reserve capacities or dispatchable power plants. For the elastic case, we still see identical prices between the LT and ST models.
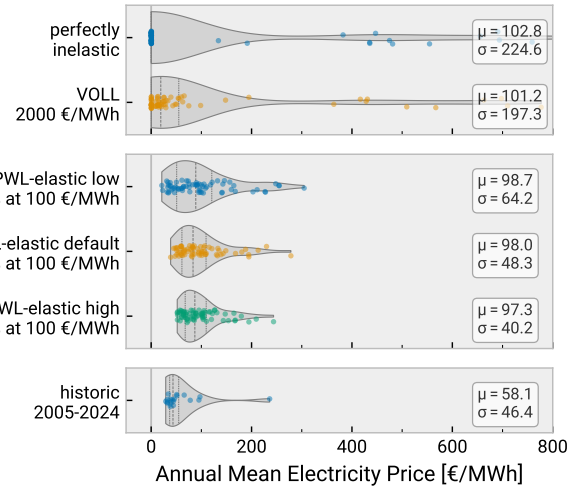

Figure 4: Distribution of average annual baseload prices in different scenarios. Violin plots show the kernel density estimate of the data. Vertical lines show the quartiles of the data. The μ signifies the mean, σ the standard deviation.
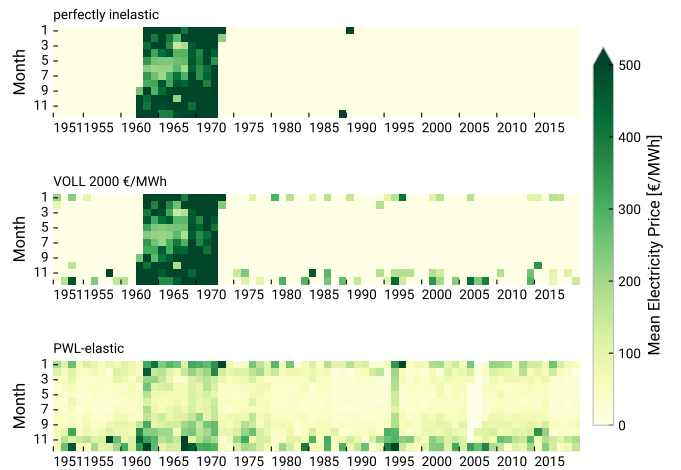
Figure 5: Heatmap of average monthly baseload prices over 70 years in different scenarios.

4.4. Inter-annual variability

One of the concerns raised about systems with high shares of variable generation is that prices might vary strongly between years as weather conditions change. The wind, in particular, is known to exhibit strong inter-annual variability (Fig. S12) [59]. Widely varying prices would make asset cost recovery uncertain and raise the risk premium for financing the assets [11, 25].

To explore this, we show in Figs. 4 and 5 the distribution of average annual and monthly baseload prices from the optimised 70-year period. The perfectly inelastic demand cases show a very high variance with a strong clustering of high prices in the 1960s. In contrast, prices cluster ever tighter for increasing elasticity and are more evenly distributed. In all cases except for fully inelastic demand, we see a seasonal pattern with higher prices in winter and broadly lower prices in summer. If we compare the results to the distribution of prices over the last 19 years [60, 61], we see a comparable range as seen in the conventional system due to fossil fuel price variability.[9]

---

[9]It should be noted that the historical wholesale market prices do not yield

Such stable prices would increase certainty and reduce risk for investors, as annual revenues would also be less volatile (Fig. S10).

4.5. Results from short-term model with myopic foresight

Until now, the short-term models have been run with perfect foresight over the same weather years used for capacity expansion planning. Now, we show results with myopic operational foresight and heuristic storage bidding as described in Section 3.3. Capacities are determined based on 35 randomly selected years in the LT model, and then operations are optimised on 35 other unseen years in the ST model. As hydrogen storage bids for ST model the we take the mean MSV of the LT model.

Fig. 6 compares price duration curves from myopic model runs (96-hour foresight, 48-hour overlap) with the LT and ST models with perfect foresight. Since the MSV is set to a constant value, there are now only two large non-zero steps in the price duration curves corresponding to the charging and discharging bids for hydrogen storage. The small intermediary steps are caused by interactions with the bids of the battery storage and the demand curve, if present (Fig. S2).

In the perfectly inelastic case, there is a large increase in hours with load-shedding going from the LT capacity expansion model to the ST operational model, since the weather years of the ST model were different to those in the LT model. With myopic foresight the heuristic storage bidding based on a constant MSV acts to regularise prices, resulting in two main non-extreme price levels besides load-shedding and zero-price hours. A constant MSV was not something found in the LT inelastic model (see Fig. 3, panel c)) but exogenously set in the model inspired by observations from the elastic case (see Fig. 3, panel d)). As a result, the monthly average baseload price distribution has a similar regularity to the case with demand elasticity (Fig. S5). Taking the constant averaged MSV blends out the volatility of the MSV formation in the absence of demand elasticity. With myopic foresight, the peak load shedding increases by 13.9% from 77.6 MW to 88.3 MW, while the average load served is just reduced by 0.5% from 99.96 MW to 99.47 MW. To compare the system operation between perfect and myopic foresight with and without demand elasticity, we refer to Fig. S11.

In the elastic case, the price duration curves are similar. Unlike in Fig. 3, the price duration curves between the LT and ST models are close but not identical. This is again because the wind and solar capacity factors are taken from different weather years. The minor differences observed between the ST models with myopic and perfect foresight outline where the heuristic storage bids under or overestimate the MSV. With myopic foresight, the average electricity price increases from 95.4 €/MWh to 126.2 €/MWh. This reflects the cost of lacking foresight. Peak demand curtailment increases by 23.2%, whereas the average load served is reduced by only 0.8%. The drop in total welfare is just 0.1%, since the welfare is dominated by the demand utility (see Table S5).

In either case, the capacity perturbations of ±5% have a similar effect as seen previously with perfect foresight in Fig. 3.

_____

full cost recovery for the assets in the system because aspects like renewable subsidies are not included.

An additional sensitivity analysis run with a shorter foresight window of 48 hours exhibits only slight differences between 96 hours and 48 hours of foresight. With longer foresight, the average load served is increased by less than 0.1%, peak load shedding is reduced by 3-7%, and average electricity prices are reduced by around 4% (Table S5).

These results highlight that long foresight horizons are not required for operating a highly renewable energy system with storage. A horizon of a few days corresponding to current forecasting skill suffices for battery scheduling and simple bidding heuristics for long-duration energy storage yield acceptable dispatch decisions. Any estimates of weather conditions further ahead will only help to improve the economic dispatch. A live website was developed by one of the authors to demonstrate how 24-hour-ahead forecasts combined with fixed hydrogen MSV are able to dispatch a fully renewable German power system over 10 years of weather data [62].

4.6. Cost recovery

Cost recovery refers to the fraction of the investment and operation costs that are recovered by the revenues from the operation of the assets. Fig. 7 shows the cost recovery for each asset in different scenarios. For the LT model, the cost recovery is perfect for all components, following the zero-profit rule shown in Brown and Reichenberg [51]. The variability of revenue from year to year is, however, much higher for the VOLL case than the PWL-elastic case (Fig. S10).

Transitioning from the LT to the ST model with perfect foresight, drastic differences are observed between demand modelling cases. The high overshoot of cost recovery rates for the perfectly inelastic case until VOLL, due to the high prices seen in Fig. 6, is not observed in the elastic case and highlights the inadequacy of modelling with perfectly inelastic demand.

For scenarios with myopic operational foresight in unseen years, the differences between inelastic and elastic demand cases are pruned by the heuristic storage bids. Especially for the elastic case, all components exceed or come close to full cost recovery. The lowest cost recovery is 97.2% for the electrolyzer. With over-capacities of 5%, cost recovery falls short and varies between 67% and 82%, incentivising market exits. The opposite holds for deficient capacities, where profits between 14% and 190% incentivise certain market entries.

All results shown in preceding Sections 4.1 to 4.6 for Germany are consistent with those observed for a more solar-dominated system in Spain and a more wind-dominated system in the United Kingdom, as shown in Appendix F.

5. Discussion

5.1. Consquences for interpreting prices in energy system models

Our results establish that the strong price bifurcations seen in many capacity expansion models are due to modelling demand without price elasticity. The combination of step-like inelastic demand curves with step-like supply curves from VRE together cause the price bifurcations. Given that today's electricity markets already feature price-sensitive demand [47], price duration curves from these models are unrealistic and should not be taken at face value.
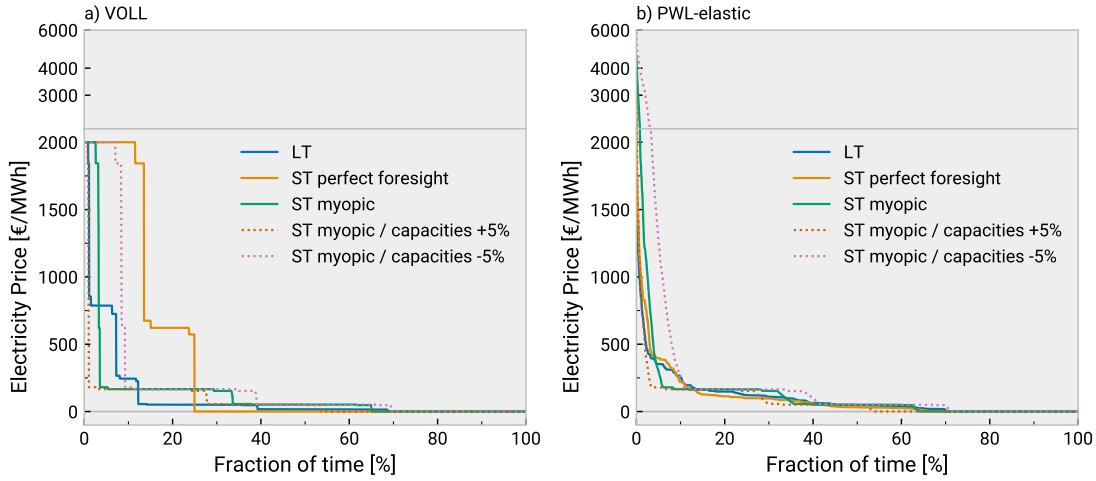
Figure 6: Price duration curves comparing short-term models with myopic foresight on unknown years, i.e. the LT and ST model take two disjunct sets of 35 weather years as input data. Blue is from the original LT model based on 35 years of data. Orange is from a ST model with optimised capacities from the LT model and perfect foresight on 35 unseen test years. Green is another ST model with myopic foresight of 96 hours and a rolling horizon overlap of 48 hours for the same unseen test years. Dotted lines add capacity perturbations of ±5% to that.
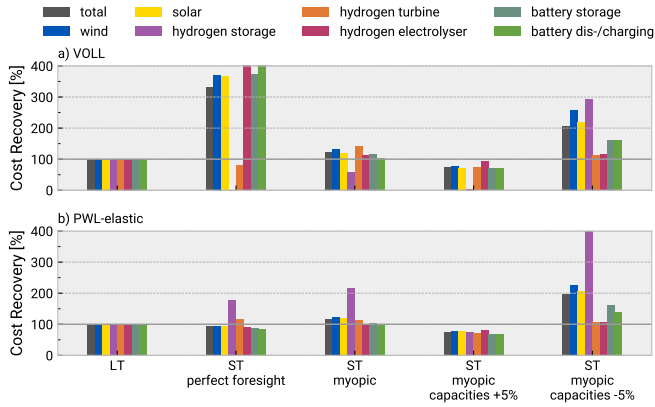

Figure 7: Cost recovery of each component as a fraction of investment, depending on demand modelling approach, operational foresight and capacity perturbations for 35-year LT plus 35-year ST optimisations.

While average prices and market values might be indicative in models with perfectly inelastic demand, the shape of the price duration curves is not stable as the number of optimised periods is changed, nor under transition from long-term to short-term modelling, nor under small perturbations of capacity, nor between different weather years. Prices either collapse to zero for extended periods or spike dramatically. The concerns in the literature, for instance, that revenues of generation and storage would be realised in just very few hours [3–6], are rooted in these observations but are, in fact, interpretations of a modelling artifact.

The short-term elasticity level observed in the German wholesale electricity market today (cf. [47]) would already be sufficient to stabilise price formation and yield a completely different picture about when revenues are made. The price formation with demand elasticity is then identical between long- and short-term models, stable under capacity perturbations, stable between between weather years, and allows for more consistent and evenly spread cost recovery.

The reason demand elasticity helps to stabilise prices is that it gives the storage a wide range of willingness-to-pay (WTP) values against which to calibrate its opportunity costs and arbitrage. With perfectly inelastic demand, the WTP jumps from zero to the value of lost load with nothing in between for the storage to bid against.

The prospect of more cross-sectoral integration further opens new opportunities for demand-side management (DSM) of electric vehicles, heat pumps, and industrial processes, beyond today's elasticity level, although inter-temporal dependencies need to be treated with care. Modelling DSM with virtual storage units is not sufficient to resolve pricing problems, as the examples above with storage show; sloped demand curves with smoothly varying WTP are what is needed for stable price formation.

5.2. Relating the modelling results to real electricity markets

Until now, we have focused mainly on explaining model results and comparing them to observations in the literature, but we believe many of our insights are transferable to real electricity markets. Our model's operation with slightly elastic demand and myopic foresight is close to how real markets function, and price formation remains stable under these conditions, as implied in Stoft's textbook [25].

Cost recovery is naturally imperfect with imperfect information. For instance, with capacities below or above the long-term equilibrium, there would be incentives for market entries or exits as asset owners would adjust their capacities to prevailing market conditions. The more regular and lower high price episodes in the elastic case would provide investors with a much more stable investment environment than the infrequent extreme high price episodes seen with the perfectly inelastic case, thus helping to avoid boom and bust cycles. The political tension between allowing scarcity pricing and remunerating dispatchable generators via capacity markets to guarantee security of supply is present in our high-VRE scenarios, just as it is in today's markets.

Our results suggest that the energy-only market remains functional in future energy systems with high VRE penetration. However, it may not be sufficient on its own to attain a low-cost renewable system. Investor risk remains thanks to uncertainties

surrounding inter-annual revenue variability, changing weather patterns due to climate change, other factors that can confound price forecasts (price cannibalisation from other renewables, CO_2 price uncertainty) as well as regulatory risks and political risks from changing climate targets. To lower investor risk and reduce financing costs, support guarantees such as investment subsidies, contracts for difference or feed-in tariffs may still be advisable [63]. The strike prices of these contracts could use the energy-only market for orientation towards efficient prices.

The assumption of a constant marginal storage value for the myopic dispatch is strong, and in reality, storage operators would adjust their bidding based on their filling state and medium to long-range weather forecasts [38]. Moreover, a flat price would mean storage operators could not perform arbitrage and recover their costs. Potentially, long-term contracts for industrial offtake or global supply (e.g. H2Global [64]) could stabilise the hydrogen price.

We also assume perfect forecast skill within the 96-hour foresight horizon. In reality, stochastic weather forecast ensembles for the next 1-2 days would guide storage owners in their bidding strategy under uncertainty [24]. However, this neglect of short-range uncertainty does not invalidate the use of bidding heuristics for long-term storage dispatch.

5.3. Comparison of chemical storage to conventional generation

In terms of their impact on price formation in electricity markets, we can compare chemical storage to conventional generation technologies. For instance, hydroelectricity shares many similarities with chemical storage. Both can provide long-duration storage that stabilises prices through long-term opportunity costs. However, unlike chemical storage, hydro-electric storage is constrained by natural inflow, self-discharge, and the fact that the storage medium cannot be traded on global markets. Hydroelectric inflow is easier to forecast on a seasonal basis that wind power fluctuations, thanks to predictable snow and rainfall patterns. On the other hand, chemical storage expansion is not geologically limited and offers more control over dimensioning and scaling.

The price of fossil fuels like gas and coal also stems from a mix of production and opportunity costs, which is similar to how the value of chemical storage is determined in our model. For hydrogen, production costs include wind and solar generation and power-to-X elements. For fossil fuels, it is land rents as well as the energy and labor costs for extraction, which may be further impacted by emission prices or scarcity prices due to supply disruptions. Similarly, prices are linked to feedstock availability for electricity production from biomass and the mining, enrichment, and fabrication of uranium into fuel rods for nuclear power. The connection to currently used fuels becomes even more apparent when considering green fuel imports for power backup, where the price is decoupled from the domestic electricity system. The price formation mechanism is then similar to that of a fossil-based system.

6. Conclusion

Our study addresses several contradictions seen in the literature about the viability of electricity markets at high penetrations of wind and solar. Our results demonstrate that price structures consisting of many zero- and high-price hours are a symptom of capacity expansion models using perfectly inelastic demand. Already a slightly elastic demand alleviates these symptoms and reduces the fraction of zero-price hours from 90% to around 30%. Besides eliminating price bifurcations, modelling demand elasticity stabilises prices between weather years, which reduces revenue risks, and aligns prices observed in long- and short-term models. Therefore, we conclude that electricity models using perfectly inelastic demand are inadequate for analysing price formation at high penetrations of variable renewable energy.

Demand elasticity not only stabilises price formation but also facilitates the operation of long-term storage with myopic foresight. The stability of the marginal values of chemical storage, which are closely linked to electricity price formation, enables the development of storage bidding strategies. Even with the simple assumption of constant storage bids, we can achieve adequate system dispatch with similar prices, reliability metrics, and cost recovery levels, with only a few days of foresight, and even if capacities do not exactly match the long-term equilibrium.

With these insights, we address many of the concerns about price formation in energy-only markets with high penetrations of wind and solar. We conclude that the energy-only market can still play a key role in coordinating future dispatch and investment given current price elasticity levels. If demand can be further flexibilised in future, this will only help to stabilise prices even more.

Code and data availability

The open source code to reproduce our experiments, including the download and installation of data and software dependencies, is available on GitHub licensed under the MIT license at https://github.com/fneum/price-formation (v0.2.0). The results data was deposited on Zenodo under the CC-BY-4.0 license at https://doi.org/10.5281/zenodo.12759247 (v0.2.0).

Author contributions

Declaration of interests

The authors declare no competing interests.

Acknowledgements

References

[1] F. Sensfuß, M. Ragwitz, M. Genoese, The merit-order effect: A detailed analysis of the price effect of renewable electricity generation on spot market prices in germany, Energy Policy 36 (8) (2008) 3086–3094. doi:10.1016/j.enpol.2008.03.035.

[2] Z. Zhou, A. Botterud, T. Levin, Price formation in zero-carbon electricity markets – fundamentals, challenges, and research needs, Renewable and Sustainable Energy Reviews 211 (2025) 115250. doi:10.1016/j.rser.2024.115250.
URL https://doi.org/10.1016/j.rser.2024.115250

[3] J. A. Taylor, S. V. Dhople, D. S. Callaway, Power systems without fuel, Renewable and Sustainable Energy Reviews 57 (2016) 1322–1336. doi:10.1016/j.rser.2015.12.083.

[4] D. S. Mallapragada, C. Junge, C. Wang, H. Pfeifenberger, P. L. Joskow, R. Schmalensee, Electricity pricing challenges in future renewables-dominant power systems, Energy Economics 126 (2023) 106981. doi:10.1016/j.eneco.2023.106981.

[5] T. Levin, J. Bistline, R. Sioshansi, W. J. Cole, J. Kwon, S. P. Burger, G. W. Crabtree, J. D. Jenkins, R. O'Neil, M. Korpås, S. Wogrin, B. F. Hobbs, R. Rosner, V. Srinivasan, A. Botterud, Energy storage solutions to decarbonize electricity through enhanced capacity expansion modelling, Nature Energy 8 (11) (2023) 1199–1208. doi:10.1038/s41560-023-01340-6.

[6] The Royal Society, Large-scale electricity storage (2023).
URL https://royalsociety.org/-/media/policy/projects/large-scale-electricity-storage/large-scale-electricity-storage-report.pdf

[7] R. Green, N. Vasilakos, Market behaviour with large amounts of intermittent generation, Energy Policy 38 (7) (2010) 3211–3220. doi:10.1016/j.enpol.2009.07.038.

[8] P. R. Brown, F. M. O'Sullivan, Spatial and temporal variation in the value of solar power across united states electricity markets, Renewable and Sustainable Energy Reviews 121 (2020) 109594. doi:https://doi.org/10.1016/j.rser.2019.109594.

[9] G. Thomaßen, C. Redl, T. Bruckner, Will the energy-only market collapse? on market dynamics in low-carbon electricity systems, Renewable and Sustainable Energy Reviews 164 (2022) 112594. doi:10.1016/j.rser.2022.112594.

[10] L. Hirth, The market value of variable renewables: The effect of solar wind power variability on their relative price, Energy Economics 38 (2013) 218–236. doi:10.1016/j.eneco.2013.02.004.

[11] J. Mays, J. Jenkins, Electricity Markets under Deep Decarbonization, SSRN Electronic Journal (2022). doi:10.2139/ssrn.4087528.

[12] F. Egli, Renewable energy investment risk: An investigation of changes over time and the underlying drivers, Energy Policy 140 (2020) 111428. doi:https://doi.org/10.1016/j.enpol.2020.111428.

[13] L. Barroso, F. D. Munoz, B. Bezerra, H. Rudnick, G. Cunha, Zero-Marginal-Cost Electricity Market Designs: Lessons Learned From Hydro Systems in Latin America Might Be Applicable for Decarbonization, IEEE Power and Energy Magazine 19 (1) (2021) 64–73. doi:10.1109/MPE.2020.3033398.

[14] J. Bistline, W. Cole, G. Damato, J. DeCarolis, W. Frazier, V. Linga, C. Marcy, C. Namovicz, K. Podkaminer, R. Sims, M. Sukunta, D. Young, Energy storage in long-term system models: A review of considerations, best practices, and research needs, Progress in Energy 2 (3) (2020) 032001. doi:10.1088/2516-1083/ab9894.

[15] O. J. Guerra, S. Dalvi, A. A. Thatte, B. Cowiestoll, J. Jorgenson, B.-M. Hodge, Towards Robust and Scalable Dispatch Modeling of Long-Duration Energy Storage (Jan. 2024). arXiv:2401.16605.

[16] B. A. Frew, M. Milligan, G. Brinkman, A. Bloom, K. Clark, P. Denholm, Revenue Sufficiency and Reliability in a Zero Marginal Cost Future: Preprint (2016).
URL https://www.nrel.gov/docs/fy17osti/66935.pdf

[17] P. Cramton, A. Ockenfels, S. Stoft, Capacity market fundamentals, Economics of Energy & Environmental Policy 2 (2) (2013) 27–46.
URL http://www.jstor.org/stable/26189455

[18] M. Hogan, Follow the missing money: Ensuring reliability at least cost to consumers in the transition to a low-carbon power system, The Electricity Journal 30 (1) (2017) 55–61. doi:10.1016/j.tej.2016.12.006.

[19] F. A. Wolak, Market Design in an Intermittent Renewable Future: Cost Recovery With Zero-Marginal-Cost Resources, IEEE Power and Energy Magazine 19 (1) (2021) 29–40. doi:10.1109/MPE.2020.3033395.

[20] D. Böttger, P. Härtel, On wholesale electricity prices and market values in a carbon-neutral energy system, Energy Economics 106 (2022) 105709. doi:10.1016/j.eneco.2021.105709.

[21] P. Härtel, M. Korpås, Demystifying market clearing and price setting effects in low-carbon energy systems, Energy Economics 93 (2021) 105051. doi:10.1016/j.eneco.2020.105051.

[22] N. Helistö, S. Johanndeiter, J. Kiviluoma, The Impact of Sector Coupling and Demand-side Flexibility on Electricity Prices in a Close to 100% Renewable Power System, in: 2023 19th International Conference on the European Energy Market (EEM), IEEE, Lappeenranta, Finland, 2023, pp. 1–6. doi:10.1109/EEM58374.2023.10161962.

[23] F. Neumann, E. Zeyen, M. Victoria, T. Brown, The potential role of a hydrogen network in Europe, Joule 7 (8) (2023) 1793–1817. doi:10.1016/j.joule.2023.06.016.

[24] P. Aaslid, M. Korpås, M. M. Belsnes, O. B. Fosso, Pricing electricity in constrained networks dominated by stochastic renewable generation and electric energy storage, Electric Power Systems Research 197 (2021) 107169. doi:10.1016/j.epsr.2021.107169.

[25] S. Stoft, Power System Economics, IEEE Press & WILEY-INTERSCIENCE, 2002. doi:10.1109/9780470545584.

[26] D. Kirschen, Demand-side view of electricity markets, IEEE Transactions on Power Systems 18 (2) (2003) 520–527. doi:10.1109/TPWRS.2003.810692.

[27] Chua-Liang Su, D. Kirschen, Quantifying the Effect of Demand Response on Electricity Markets, IEEE Transactions on Power Systems 24 (3) (2009) 1199–1207. doi:10.1109/TPWRS.2009.2023259.

[28] G. W. Leslie, D. I. Stern, A. Shanker, M. T. Hogan, Designing electricity markets for high penetrations of zero or low marginal cost intermittent energy sources, The Electricity Journal 33 (9) (2020) 106847. doi:10.1016/j.tej.2020.106847.

[29] P. Massé, Les réserves et la régulation de l'avenir dans la vie économique. 1.2., Vol. 1-2 of Actualités scientifiques et industrielles, Hermann, Paris, 1946.

[30] R. Bellman, Dynamic Programming, Princeton University Press, Princeton, NJ, 1957.
URL https://gwern.net/doc/statistics/decision/1957-bellman-dynamicprogramming.pdf

[31] J. D. C. Little, The use of storage water in a hydroelectric system, Journal of the Operations Research Society of America 3 (2) (1955) 187–197. doi:10.1287/opre.3.2.187.

[32] T. C. Koopmans, Water storage policy in a simplified hydroelectric system, Cowles Foundation Discussion Papers 243 (1957).
URL https://elischolar.library.yale.edu/cowles-discussion-paper-series/243/

[33] V. Hveding, Digital simulation techniques in power system planning, Economics of Planning 8 (1-2) (1968) 118–139. doi:10.1007/bf02481379.

[34] P. Lederer, P. Torrion, J. Bouttes, Overall control of an electricity supply and demand system: A global feedback for the French system, in: System Modelling and Optimization, Springer, 1984, pp. 609–617. doi:10.1007/BFb0008934.

[35] T. A. Rotting, A. Gjelsvik, Stochastic dual dynamic programming for seasonal scheduling in the norwegian power system, IEEE Transactions on Power Systems 7 (1) (1992) 273–279. doi:10.1109/59.141714.

[36] O. Fosso, A. Gjelsvik, A. Haugstad, B. Mo, I. Wangensteen, Generation scheduling in a deregulated system. The Norwegian case, IEEE Transactions on Power Systems 14 (1) (1999) 75–81. doi:10.1109/59.744487.

[37] C. Crampes, J.-M. Trochet, Economics of stationary electricity storage with various charge and discharge durations, Journal of Energy Storage 24 (2019) 100746. doi:10.1016/j.est.2019.04.020.

[38] M.-A. D. la Tour, Towards a decarbonized energy system in europe in 2050: Impact of vector coupling and renewable deployment limits, Phd thesis, École doctorale de l'École des hautes études en sciences sociales (2023).
URL https://theses.fr/2023EHES0014

[39] K. Ward, I. Staffell, Simulating price-aware electricity storage without linear optimisation, Journal of Energy Storage 20 (2018) 78–91. doi:10.1016/j.est.2018.08.022.

[40] K. Ward, R. Green, I. Staffell, Getting prices right in structural electricity market models, Energy Policy 129 (2019) 1190–1206. doi:10.1016/j.enpol.2019.01.077.

[41] M. Korpås, A. Botterud, Optimality conditions and cost recovery in electricity markets with variable renewable energy and energy storage,

Tech. rep. (2020).
URL http://ceepr.mit.edu/files/papers/2020-005.pdf

[42] G. Tarel, M. Korpås, A. Botterud, Long-term equilibrium in electricity markets with renewables and energy storage only, Energy Systems (Apr 2024). doi:10.1007/s12667-024-00654-y.

[43] W. Antweiler, F. Müsgens, The new merit order: The viability of energy-only electricity markets with only intermittent renewable energy sources and grid-scale storage, Tech. rep. (2024). doi:10.2139/ssrn.4702939.

[44] T. Ekholm, V. Virasjoki, Pricing and competition with 100% variable renewable energy and storage, The Energy Journal 42 (1_suppl) (2021) 1–18. doi:10.5547/01956574.42.S12.tekh.

[45] C. De Jonghe, B. F. Hobbs, R. Belmans, Optimal generation mix with short-term demand response and wind penetration, IEEE Transactions on Power Systems 27 (2) (2012) 830–839. doi:10.1109/TPWRS.2011.2174257.

[46] E. Adachi, E. Brock, R. Kravis, Understanding price formation in grids transitioning to zero marginal cost generation, in: 2024 IEEE Power and Energy Conference at Illinois (PECI), 2024, pp. 1–6. doi:10.1109/PECI61370.2024.10525256.

[47] L. Hirth, T. M. Khanna, O. Ruhnau, How aggregate electricity demand responds to hourly wholesale price fluctuations, Energy Economics 135 (2024) 107652. doi:10.1016/j.eneco.2024.107652.

[48] F. Arnold, On the functional form of short-term electricity demand response - Insights from high-price years in Germany, EWI Working Paper 23/06, Institute of Energy Economics at the University of Cologne (EWI), Cologne (2023).
URL https://hdl.handle.net/10419/286380

[49] Gurobi, Gurobi optimization v11.0.2 (2024).
URL https://www.gurobi.com/

[50] S. Boyd, L. Vandenberghe, Convex Optimization, Cambridge University Press, 2004.
URL https://stanford.edu/~boyd/cvxbook/

[51] T. Brown, L. Reichenberg, Decreasing market value of variable renewables can be avoided by policy action, Energy Economics 100 (2021) 105354. doi:10.1016/j.eneco.2021.105354.

[52] D. R. Biggar, M. R. Hesamzadeh (Eds.), The Economics of Electricity Markets, John Wiley & Sons Ltd, 2014. doi:10.1002/9781118775745.
URL https://doi.org/10.1002/9781118775745

[53] H. C. Bloomfield, D. J. Brayshaw, M. Deakin, D. Greenwood, Hourly historical and near-future weather and climate variables for energy system modelling, Earth System Science Data 14 (6) (2022) 2749–2766. doi:10.5194/essd-14-2749-2022.

[54] T. Brown, J. Hörsch, D. Schlachtberger, PyPSA: Python for Power System Analysis, Journal of Open Research Software 6 (4) (2018). doi:10.5334/jors.188.

[55] F. Hofmann, Linopy: Linear optimization with n-dimensional labeled variables, Journal of Open Source Software 8 (84) (2023) 4823. doi:10.21105/joss.04823.

[56] T. Brown, D. Schlachtberger, A. Kies, M. Greiner, Synergies of sector coupling and transmission extension in a cost-optimised, highly renewable European energy system, Energy 160 (2018) 720–730. doi:10.1016/j.energy.2018.06.222.

[57] P. Bauer, A. Thorpe, G. Brunet, The quiet revolution of numerical weather prediction, Nature 525 (2015) 47–55. doi:10.1038/nature14956.

[58] L. Magnusson, D. Ackerley, Y. Bouteloup, J.-H. Chen, J. Doyle, P. Earnshaw, Y. C. Kwon, M. Köhler, S. T. K. Lang, Y.-J. Lim, M. Matsueda, T. Matsunobu, R. McTaggart-Cowan, A. Reinecke, M. Yamaguchi, L. Zhou, Skill of medium-range forecast models using the same initial conditions, Bulletin of the American Meteorological Society 103 (9) (2022). doi:10.1175/BAMS-D-21-0234.1.

[59] S. C. Pryor, R. J. Barthelmie, J. T. Schoof, Inter-annual variability of wind indices across europe, Wind Energy 9 (1-2) (2006) 27–38. doi:https://doi.org/10.1002/we.178.

[60] J. Muehlenpfordt, Open Power System Data: Time series, version 2020-10-06 supplemented with version 2019-06-05. (2020). doi:10.25832/time_series/2020-10-06.

[61] ENTSO-E, ENTSO-E Transparency Platform: Day ahead prices (2024).
URL https://transparency.entsoe.eu/transmission-domain/r2/dayAheadPrices/show

[62] T. Brown, Future power systems with today's weather (2024).
URL https://model.energy/future/

[63] K. Neuhoff, N. May, J. C. Richstein, Financing renewables in the age of falling technology costs, Resource and Energy Economics 70 (2022) 101330. doi:10.1016/j.reseneeco.2022.101330.

[64] H2Global Foundation, H2Global (2024).
URL https://www.h2-global.org/

[65] Danish Energy Agency, Technology catalogues (2024).
URL https://ens.dk/en/our-services/technology-catalogues

Appendix A. Substitutions to improve numerics

Many of our initial runs with VOLL or demand elasticity represented as outlined in Eq. (1) were numerically unstable and did not converge when many weather years were included. We found that making the substitutions $d_c \to D_c - g_c$ for VOLL and $d_c \to a_c/b_c - g_c$ for demand elasticity drastically improved the convergence of the model while yielding the identical results, as they remove large constants from the objective.

The suggested substitutions switch from modelling the demand as a decision variable to modelling load shedding from fixed peak consumption (D_c or a_c/b_c) as a decision variable. In terms of the objective function, it yields for VOLL

$$
\begin{aligned}
U_c(d_c) &= V_c d_c \\
U_c(g_c) &= V_c(D_c - g_c) = V_c D_c - V_c g_c,
\end{aligned}
\tag{A.1}
$$

and for the elastic case

$$
\begin{aligned}
U_c(d_c) &= a_c d_c - \frac{b_c}{2} d_c^2 \\
U_c(g_c) &= a_c \left(\frac{a_c}{b_c} - g_c \right) - \frac{b_c}{2} \left(\frac{a_c}{b_c} - g_c \right)^2 \\
&= \frac{a_c^2}{b_c} - a_c g_c - \frac{b_c}{2} \left(\frac{a_c^2}{b_c^2} - 2\frac{a_c}{b_c} g_c + g_c^2 \right) \\
&= \frac{a_c^2}{b_c} - a_c g_c - \frac{a_c^2}{2b_c} + a_c g_c - \frac{b_c}{2} g_c^2 \\
&= \frac{a_c^2}{2b_c} - \frac{b_c}{2} g_c^2.
\end{aligned}
\tag{A.2}
$$

Since the constant terms $V_c D_c$ and $a_c^2/2b_c$, which represent the welfare under the demand curve, do not affect the optimisation, we can drop them from the objective function. What remains is a load-shedding generator with the cost curve $C_c(g_c) = V_c g_c$ or $C_c(g_c) = \frac{b_c}{2} g_c^2$ for the elastic case. In addition, a fixed demand of D_c or a_c/b_c, respectively, needs to be added to the model.

This substitution trick can also be generalised for piecewise-linear demand curves with segments c, where the demand curves are not zero at a_c/b_c. We now apply the more general substitution $d_c \to D_c - g_c$ for each segment c.

$$
\begin{aligned}
U_c(d_c) &= a_c d_c - \frac{b_c}{2} d_c^2 \\
U_c(g_c) &= a_c (D_c - g_c) - \frac{b_c}{2} (D_c - g_c)^2 \\
&= a_c D_c - a_c g_c - \frac{b_c}{2} \left(D_c^2 - 2D_c g_c + g_c^2 \right) \\
&= a_d D_c - a_c g_c - \frac{b_c D_c}{2} + b_c D_c g_c - \frac{b_c}{2} g_c^2 \\
&= \left(a_c D_c - \frac{b_c D_c}{2} \right) + (b_c D_c - a_c) g_c + \left(\frac{-b_c}{2} \right) g_c^2,
\end{aligned}
\tag{A.3}
$$

resulting in load-shedding generators with a cost curve

$$
C_c(g_c) = (a_c - b_c D_c) g_c + \frac{b_c}{2} g_c^2,
\tag{A.4}
$$

again dropping the constant term from the objective function.

Appendix B. Including cross-elasticity terms

To account for how demand changes in one hour affect the demand curve in other hours, we extend the quadratic utility term in the objective function to include cross-elasticity terms:

$$U_c(d_{c,t}) = \sum_t \left(a_c d_{c,t} - \frac{b_c}{2} d_{c,t}^2 + \sum_k \frac{\gamma_{c,t,k}}{2} d_{c,t} d_{c,k} \right) \tag{B.1}$$

where $\gamma_{c,t,k}$ represents the cross-elasticity between hours t and k for segment c. The factor $\frac{1}{2}$ appears because each cross-term appears twice in the summation. The cross-elasticity coefficient is symmetric ($\gamma_{c,t,k} = \gamma_{c,k,t}$) and is only non-zero for adjacent hours within a specified time window:

$$\gamma_{c,t,k} = \begin{cases} \gamma_c & \text{if } |t - k| \leq \hat{T} \text{ and } t \neq k \\ 0 & \text{otherwise} \end{cases} \tag{B.2}$$

where $\hat{T}$ is the maximum difference in time steps for considering cross-elasticity effects and γ_c is chosen proportionally to b_c. For each demand segment c, we use $\gamma_c = \frac{b_c}{16}$ in the default case to ensure cross-effects do not dominate own-price elasticity. We also choose as default $\hat{T} = 4$ hours. The diagonal elements ($t = k$) are zero since own-price effects are already captured by the quadratic term with coefficient b_c.

This approach means that if demand in hour t decreases by 1 MW, the willingness to pay in all hours k where $|t - k| \leq \hat{T}$ increases by γ_c €/MWh, reflecting the increased need to consume in those hours to maintain the same total consumption level. The cross-elasticity does not change the price elasticity itself; the demand curve shifts up in those hours, but its slope (elasticity) stays the same. The objective function remains concave with the inclusion of cross-elasticity terms as long as γ_c is small enough, such that we do not expect a strong computational impact.

For numerical stability, we apply the same substitution as in Appendix A, replacing $d_{c,t} \to D_c - g_{c,t}$ where $D_c = a_c/b_c$. For the cross-elastic terms, this yields:

$$\sum_k \left(\frac{\gamma_{c,t,k}}{2} d_{c,t} d_{c,k} \right) = \sum_k \left(\frac{\gamma_{c,t,k}}{2} (D_c - g_{c,t})(D_c - g_{c,k}) \right)$$

$$= \sum_k \left(\frac{\gamma_{c,t,k}}{2} (D_c^2 - D_c g_{c,t} - D_c g_{c,k} + g_{c,t} g_{c,k}) \right)$$

$$= \sum_k \left(\frac{D_c^2 \gamma_{c,t,k}}{2} - \frac{D_c \gamma_{c,t,k}}{2} g_{c,t} - \frac{D_c \gamma_{c,t,k}}{2} g_{c,k} + \frac{\gamma_{c,t,k}}{2} g_{c,t} g_{c,k} \right) \tag{B.3}$$

$$\tag{B.4}$$

The constant terms $\sum_k D_c^2 \gamma_{c,t,k}/2$ can be dropped from the objective function. The remaining terms are added to the objective function as cost terms of load shedding generators $g_{c,t}$ for cost minimisation, analogous to Appendix A:

$$\sum_k \left(\frac{D_c \gamma_{c,t,k}}{2} g_{c,t} + \frac{D_c \gamma_{c,t,k}}{2} g_{c,k} - \frac{\gamma_{c,t,k}}{2} g_{c,t} g_{c,k} \right). \tag{B.5}$$

In Fig. S1a, we compare price duration curves for different cases with and without cross-elasticity terms. We see that across a range of different parameterisations, the cross-elasticity terms lead to higher peak prices and more price discontinuities. With only own-price elasticity, a demand reduction in a high price hour directly reduces the price. There is no interaction with other hours that could counteract this price-moderating effect. With cross-elastic terms, demand shifts can create new price pressures in adjacent hours. This results in higher peak price levels, lower overall demand reduction, and larger backup capacities. For $\gamma_c = b_c/16$ and $\hat{T} = 4$h, the capacity of hydrogen turbine increases by 20% to 56 MW$_{\text{el}}$ compared to the 46 MW$_{\text{el}}$ without cross-elasticity. Larger cross-elastic terms further intensify the price spikes and discontinuities. The high price hours are those when the output of the hydrogen turbines is at full capacity. Because it is unclear what values for cross-elasticity are realistic, we show results for a selection of cross-elastic terms while still maintaining a concave objective function.

In Fig. S1b, we show that cross-elastic terms can also affect the price identity between LT and ST models with identical capacities. With only own-price elasticity, we have a strict monotonic relationship between price and demand in each hour. As demonstrated in Section 2.3, this leads to a unique solution and identical prices between LT and ST models. When we add cross-price elasticities, demand in each hour depends on prices in multiple hours. This creates, in principle, multiple valid ways to distribute demand across hours while achieving the same total welfare. The LT and ST models can choose different temporal distributions of demand/prices that are equally optimal (i.e. they achieve exactly the same level of utility and supply the same total demand). The results in Fig. S1b for Germany and also Figs. S19 and S20 for Spain and the UK show that, while prices align in the vast majority of hours, the price duration curves are no longer completely identical between LT and ST models.
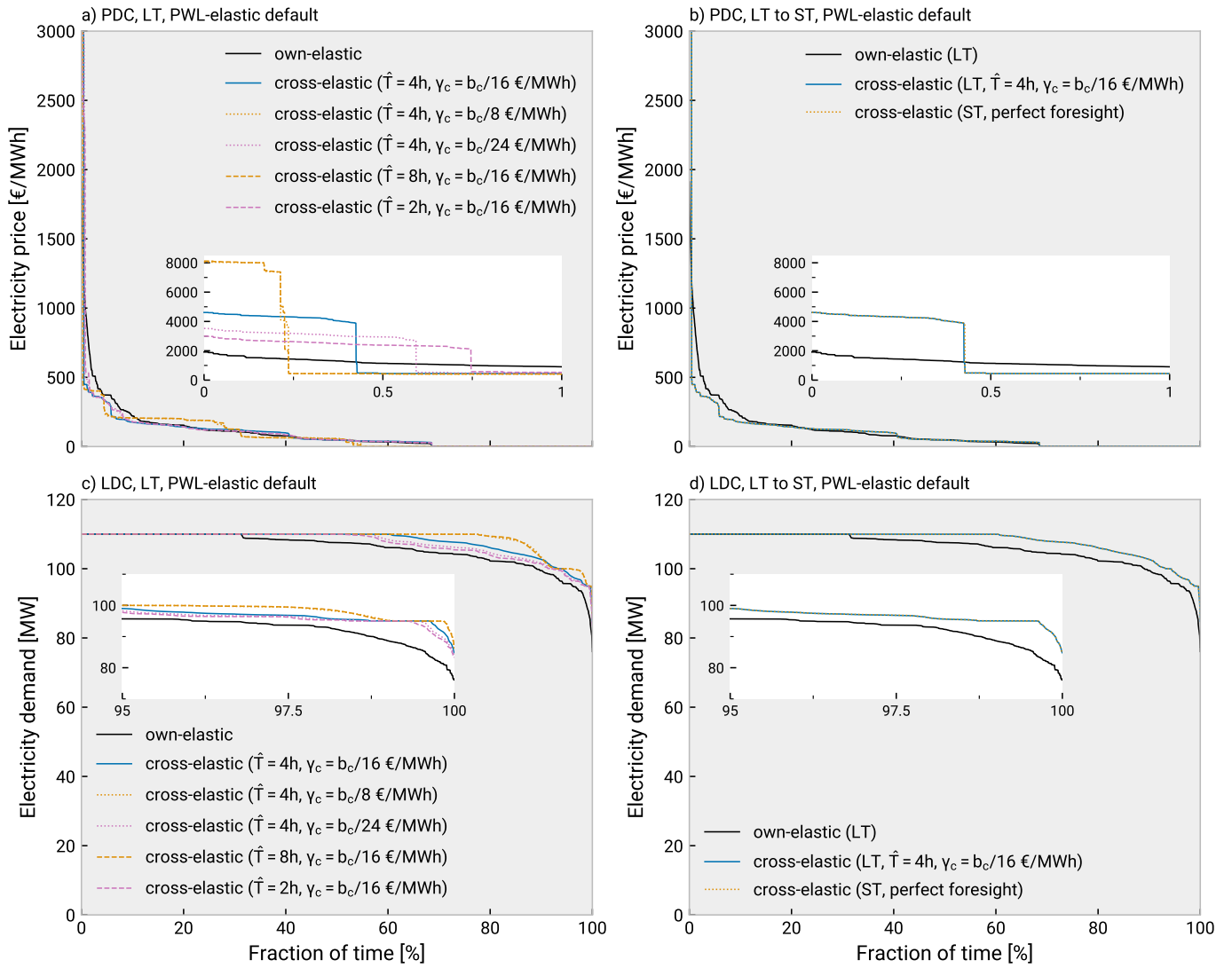
Figure S1: Price and load duration curves for LT and ST models with cross-elasticity terms alongside piecewise-linear own-elastic demand. Panel a) shows the effect of varyign cross-elasticity coefficients γ_c and $\hat{T}$ on the price duration curve (PDC). Panel b) shows the effect of moving from LT to ST models with cross-elasticity terms on the prices. Panels c) and d) show the load duration curves (LDC) corresponding to the price duration curves shown in panels a) and b), respectively.

Appendix C. Technology data

Table S1 shows the techno-economic assumptions used in the model.

Table S1: Overview of techno-economic assumptions, mostly based on projections for the year 2030 from the Danish Energy Agency (DEA) [65]. The currency year is 2020. A uniform discount rate of 7% is assumed. Efficiencies are shown as one-way efficiencies. Fixed operation and maintenance cost are given as a percentage of the overnight investment cost per year.

Technology	Investment Cost		Fixed Operation & Maintenance	Efficiency	Lifetime
Onshore wind	1095.9	€/kW	1.22 %/a	–	30 a
Solar photovoltaics	543.3	€/kW	1.95 %/a	–	40 a
Battery inverter	169.3	€/kW	0.34 %/a	96.0%	10 a
Battery storage	150.3	€/kWh	–	–	25 a
Electrolysis	1500.0	€/kW$_{el}$	4.00 %/a	62.2%	25 a
H$_2$ turbine	1164.0	€/kW$_{el}$	5.00 %/a	50.0%	10 a
H$_2$ cavern storage	0.15	€/kWh	–	–	100 a

Appendix D. Selection of years in random sequence

The 70 years (1951-2020) we consider are first put in a random sequence using the Fischer-Yates shuffle. The underlying Mersenne Twister random number generator is initialised with the seed 123. For our myopic dispatch analysis in Section 3.3, where an LT model is first optimised on 35 years and then a ST model is run on the remaining 35 years, we take the last 35 years from the shuffled list for the LT model and the first 35 years for the ST model. The resulting years for each model are given in Table S2. For Fig. 3, where the number of years N in the simulation is increased step by step, we use the N last entries in the shuffled list of weather years. That means, for instance, that the years in the 4-year run are included in the 16-year run. The shuffled sequence is not put in chronological order. The resulting years for each case are given in Table S3. All other 70-year runs use the weather years 1951 to 2020 in chronological order. All other single-year runs use 2020 as the weather year.

Model	Years (in order)
LT model (35 years)	1960, 1996, 1953, 2020, 1979, 1971, 1998, 2014, 2013, 1989, 1956, 1978, 1951, 2006, 1966, 1995, 2004, 2011, 2009, 1959, 1961, 1954, 2005, 2010, 1972, 1986, 2016, 1975, 1955, 1964, 2019, 2003, 1962, 1985, 1957
ST model (35 years)	2007, 1987, 1974, 1976, 1981, 1993, 1988, 2015, 1958, 2018, 1970, 1990, 1968, 1991, 1965, 1963, 1992, 1973, 2002, 2001, 1982, 1967, 1999, 2017, 1994, 1984, 1977, 1980, 2012, 2000, 1983, 1997, 1969, 1952, 2008

Table S2: Years used in the 35-year LT and ST models.

Number of years	Years (in order)
1 year	1957
4 years	2003, 1962, 1985, 1957
16 years	1959, 1961, 1954, 2005, 2010, 1972, 1986, 2016, 1975, 1955, 1964, 2019, 2003, 1962, 1985, 1957
32 years	2020, 1979, 1971, 1998, 2014, 2013, 1989, 1956, 1978, 1951, 2006, 1966, 1995, 2004, 2011, 2009, 1959, 1961, 1954, 2005, 2010, 1972, 1986, 2016, 1975, 1955, 1964, 2019, 2003, 1962, 1985, 1957
48 years	1999, 2017, 1994, 1984, 1977, 1980, 2012, 2000, 1983, 1997, 1969, 1952, 2008, 1960, 1996, 1953, 2020, 1979, 1971, 1998, 2014, 2013, 1989, 1956, 1978, 1951, 2006, 1966, 1995, 2004, 2011, 2009, 1959, 1961, 1954, 2005, 2010, 1972, 1986, 2016, 1975, 1955, 1964, 2019, 2003, 1962, 1985, 1957
70 years	2007, 1987, 1974, 1976, 1981, 1993, 1988, 2015, 1958, 2018, 1970, 1990, 1968, 1991, 1965, 1963, 1992, 1973, 2002, 2001, 1982, 1967, 1999, 2017, 1994, 1984, 1977, 1980, 2012, 2000, 1983, 1997, 1969, 1952, 2008, 1960, 1996, 1953, 2020, 1979, 1971, 1998, 2014, 2013, 1989, 1956, 1978, 1951, 2006, 1966, 1995, 2004, 2011, 2009, 1959, 1961, 1954, 2005, 2010, 1972, 1986, 2016, 1975, 1955, 1964, 2019, 2003, 1962, 1985, 1957

Table S3: Weather years for scenarios with incremental number of years represented.

Appendix E. Additional figures

In this section we show in a simplified case for a single year how prices duration curves are built up (Fig. S2), a sensitivity analysis for how price duration curves change if some dispatchable conventional is retained in the market (Fig. S3) or when some reserve storage discharging capacity is procured out-of-market (Fig. S4). We also show the heatmaps of average monthly baseload prices for different demand modelling scenarios with perfect and myopic foresight on 35 unseen test weather years (Fig. S5). Load duration curves corresponding to the scenarios shown in Figs. 3 and 6 respectively are shown in Figs. S6 and S7. In Fig. S8, we show in which time periods demand reductions of varying magnitude are located. In Fig. S9, we show the revenues of different system components by price band, similar to Mallapragada et al. [4]. In Fig. S10, we show the distribution of annual revenues for different system components. In Fig. S11, we illustrate the operation of the electricity system as balance time series for different demand modelling and operational foresight cases. Finally, Fig. S12 shows the relation between hourly marginal storage values and the average annual capacity factor anomaly of wind and solar.
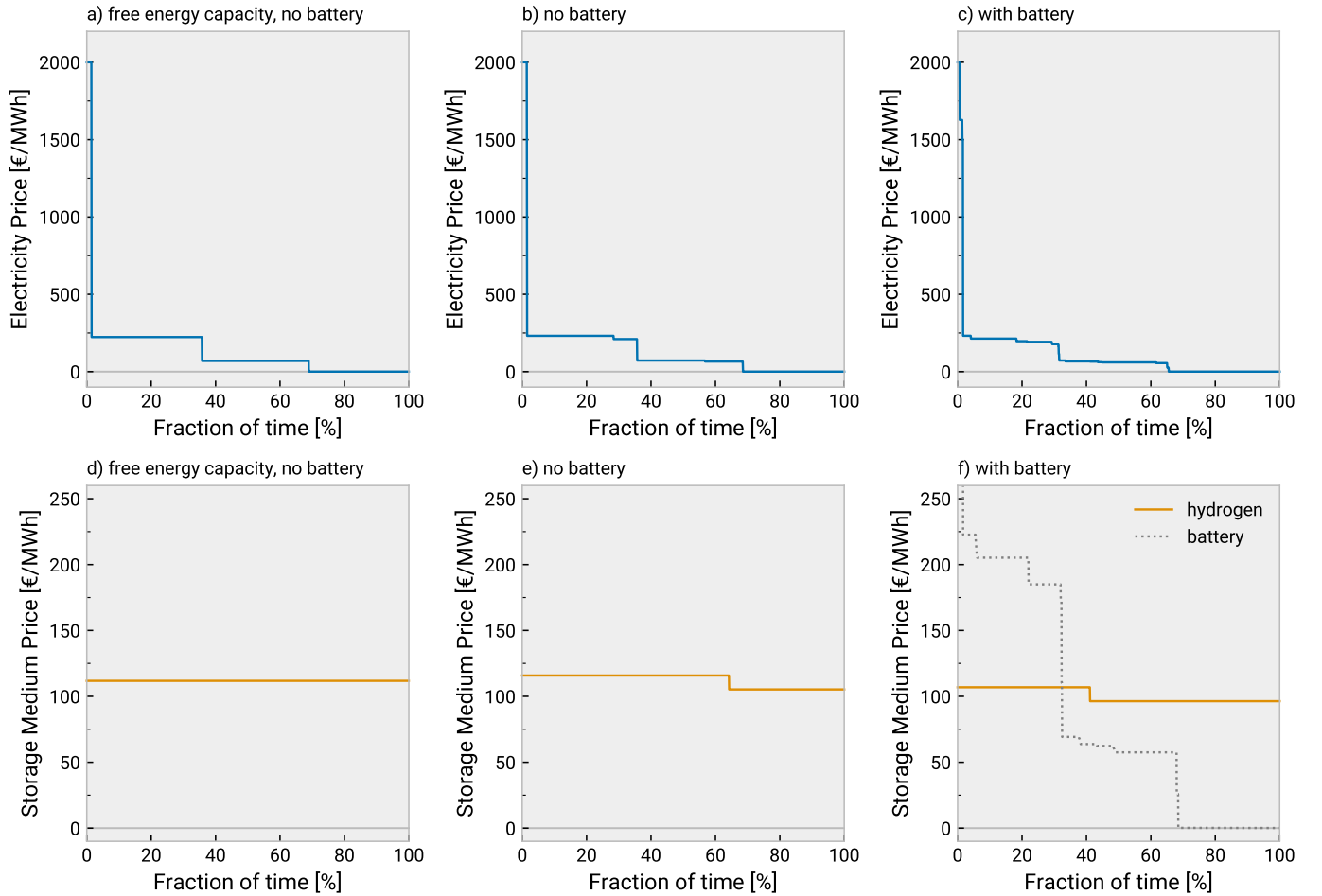
Figure S2: Price duration and marginal storage value duration curves for a single year (2020) with perfectly inelastic demand up to a VOLL of 2000 €/MWh. Case a)/d) only has VRE (wind and solar) and unconstrained hydrogen storage without energy capacity cost. Since the storage itself does not need to recover any investment costs through price arbitrage, we see a uniform hydrogen price. This translates to four price levels in the electricity price duration curve; for VRE, VOLL, storage charging and discharging. Case b)/e) includes energy capacity costs for the hydrogen storage, creating two price levels for hydrogen such that the storage energy capacity can earn a revenue to recover its costs. This carries over to the electricity price duration curve, where there are now six price levels; two levels each for storage charging and discharging. Case c)/f) additional includes battery storage, which leads to a more complex price duration curve with the previous six major price levels and small steps at their boundary, resulting from the battery's arbitrage operations.
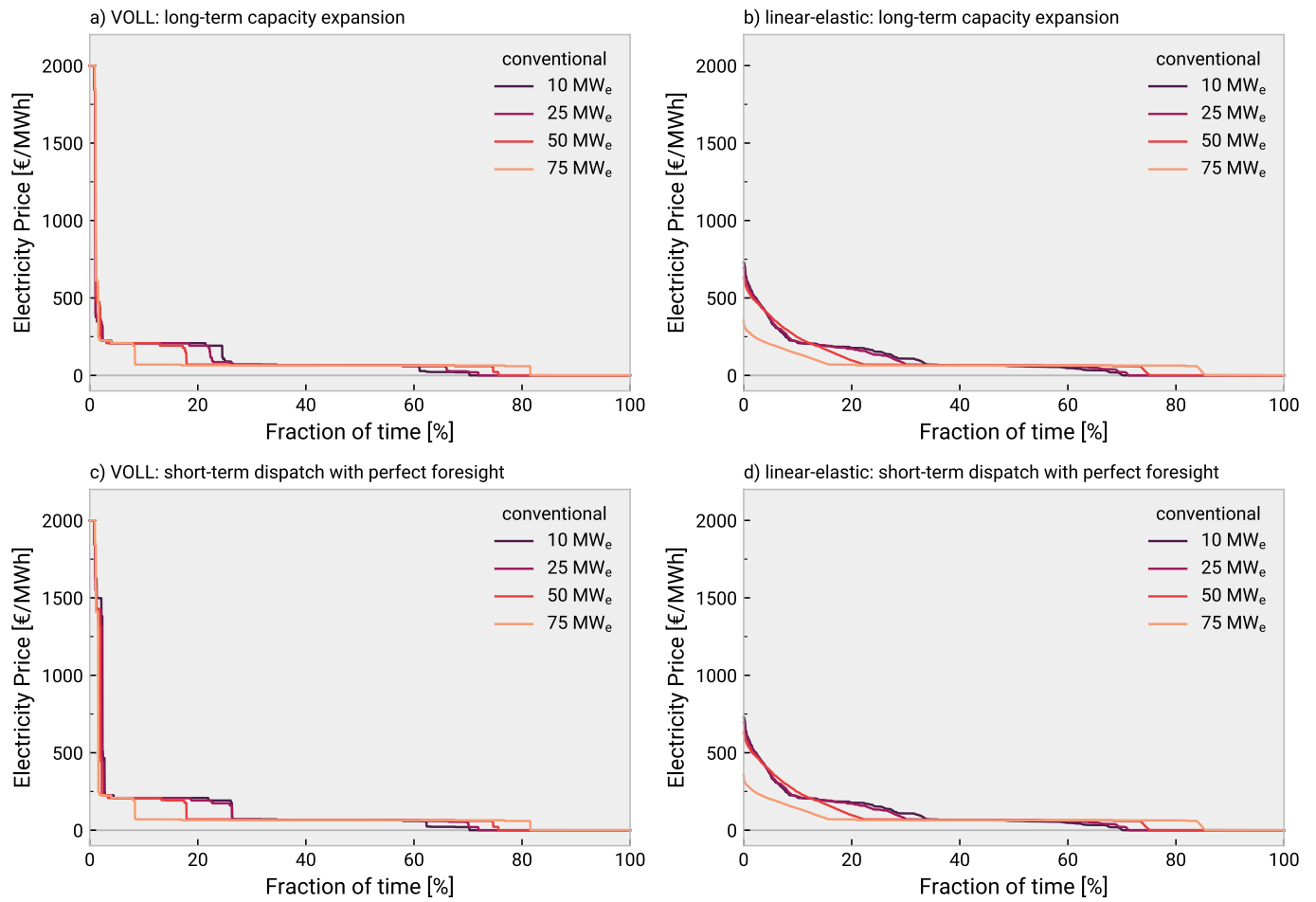
Figure S3: Sensitivity of price duration curves to dispatchable conventional capacity in LT and ST model with 20 weather years from 2001-2020. Dispatchable electricity cost is 64.7 €/MWh creating an additional price level in the centre of the price duration curve that widens with increasing dispatchable capacity. VOLL is 2000 €/MWh. Linear elastic demand run with parameters $a = 2000$ and $b = 10$. Overall, our findings remain unchanged with dispatchable conventional capacity in the system.
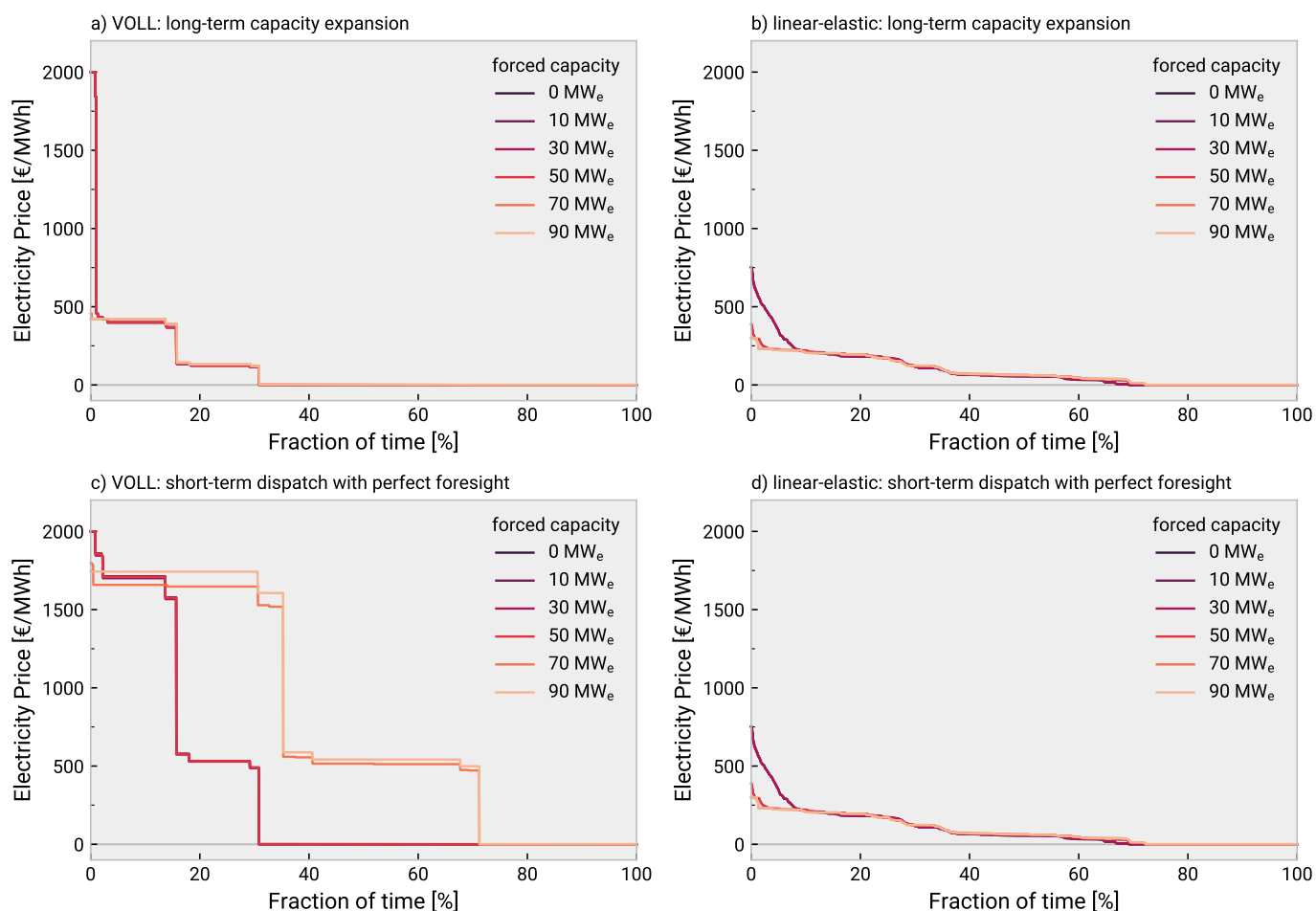
Figure S4: Sensitivity of price duration curves to reserve capacity in LT and ST model with 20 weather years from 2001-2020. Reserve hydrogen storage discharging capacity is forced into the system by setting a minimum capacity for the hydrogen turbine to electricity. VOLL is 2000 €/MWh. Linear elastic demand run with parameters $a = 2000$ and $b = 10$. Overall, our findings remain unchanged with reserve capacity procured outside the market. For the elastic case, we have price identity between LT and ST model. For the perfectly inelastic case, the prices rise drastically in the ST model compared to the LT model as the reserve capacity is increased. The forced additional dispatch capacity adds scarcity prices to the storage medium, which is then reflected in the electricity prices. As this setup is outside the model equilibrium, total welfare is lower. These price increases are not seen in the elastic case, where the prices remain stable because the demand willingness to pay sets the price rather than the storage bid.
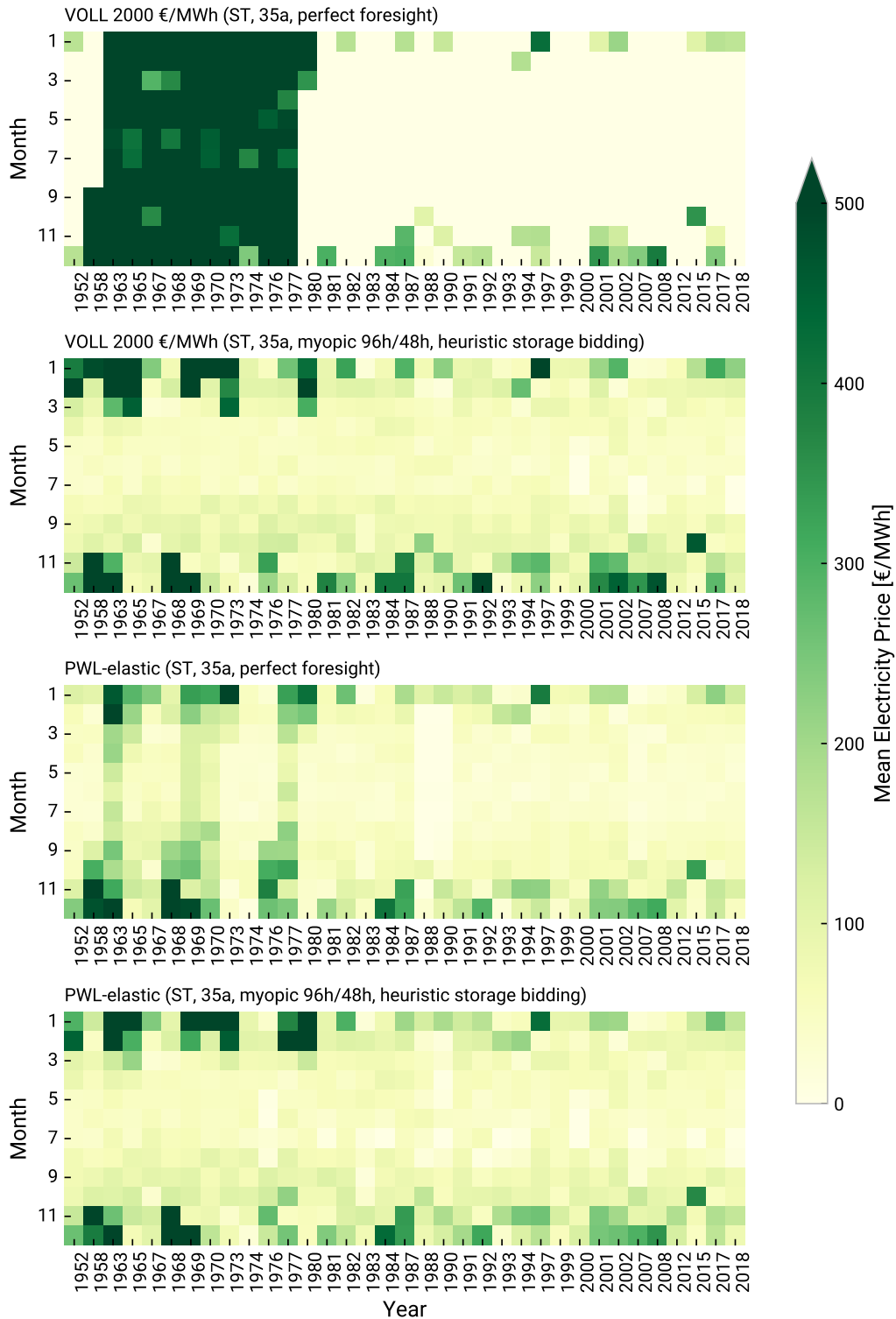
Figure S5: Heatmap of average monthly baseload prices over 35 unseen weather years for different demand modelling scenarios with perfect and myopic foresight with heuristic storage bidding. Years between 1951 and 2020 not indexed were used for the corresponding LT model.
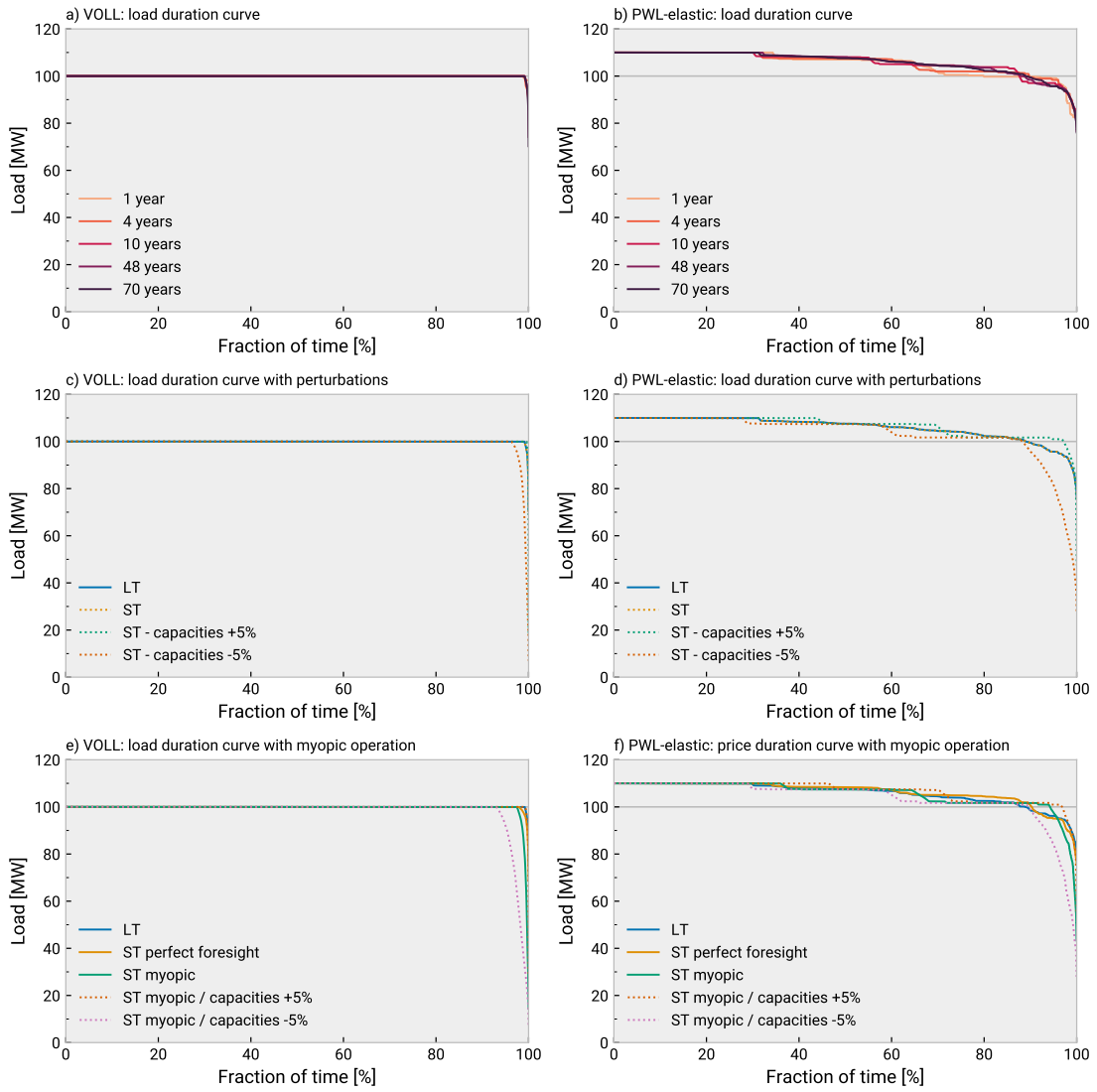
Figure S6: Load duration curves for Germany for cases analogous to Fig. 3.
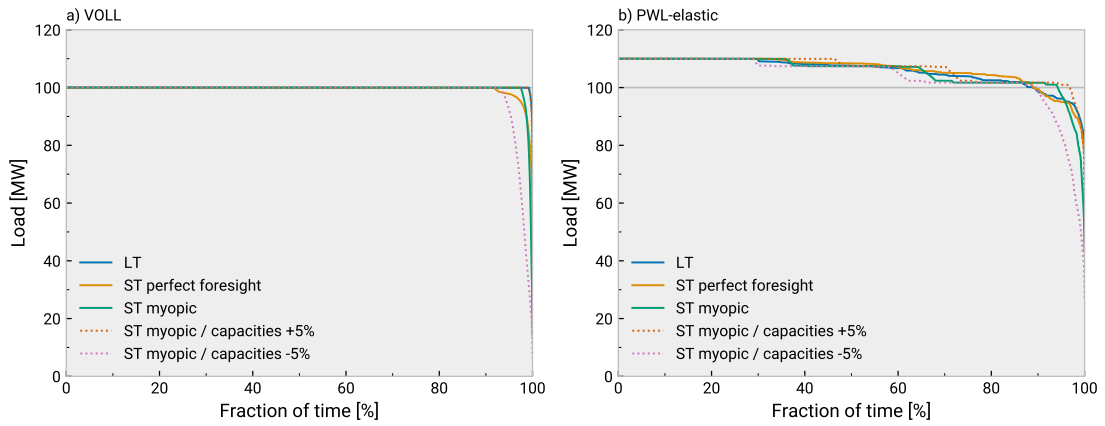
Figure S7: Load duration curves for Germany for cases with myopic foresight analogous to Fig. 6.
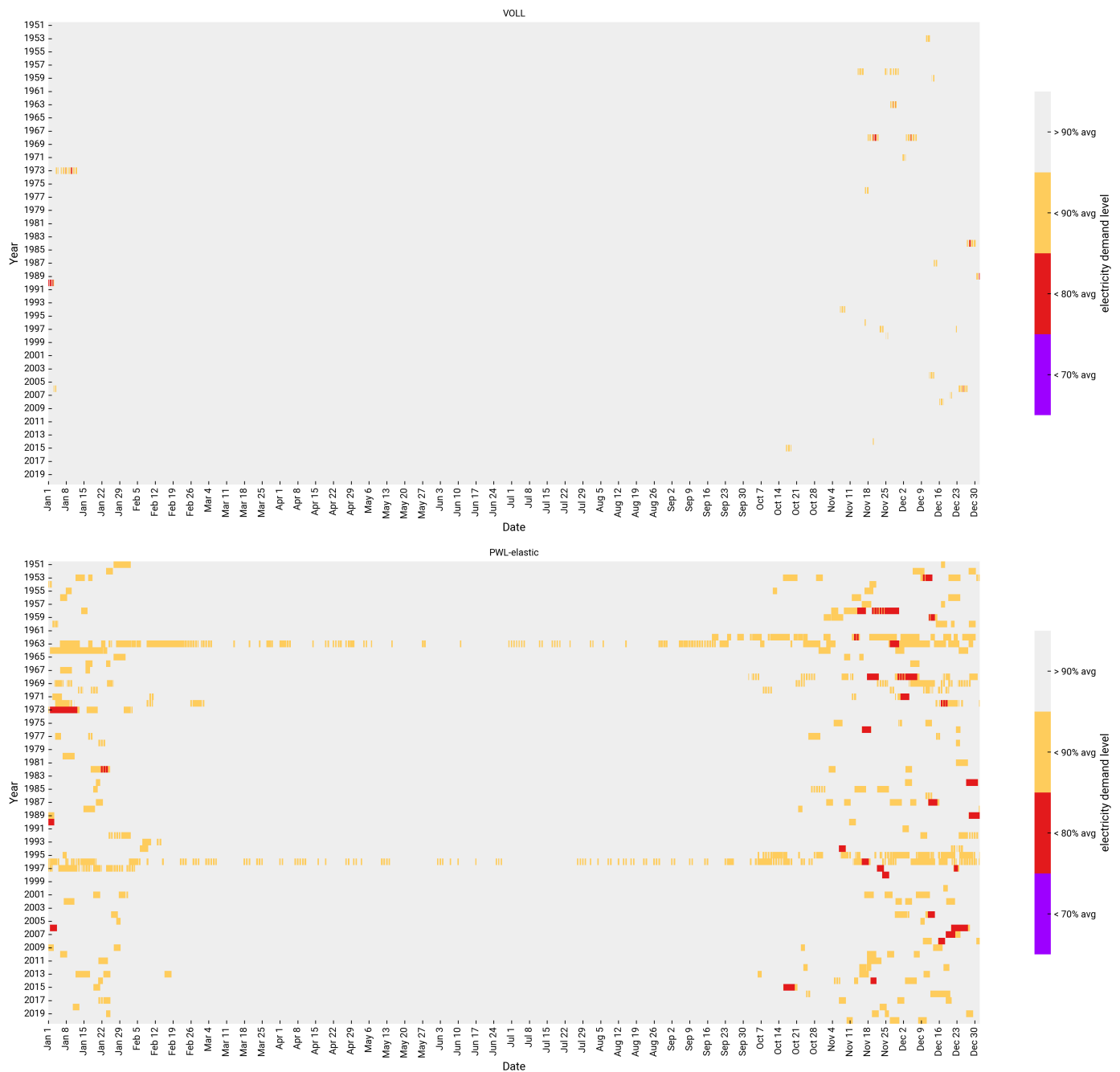
Figure S8: Time periods with demand reductions of 90%, 80%, 70% and higher, shown for different demand modelling scenarios.
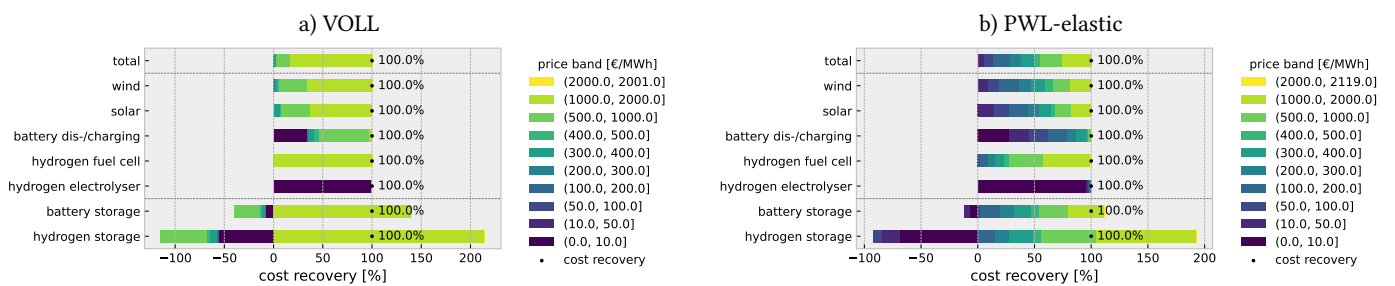
Figure S9: Cost recovery of each component by price band. In the perfectly inelastic case, most of the revenue is made in the price band of 1000-2000 €/MWh, while in the elastic case the revenue is more evenly distributed across different price bands. In both cases, storage buys electricity in low-priced hours and sells it in high-priced hours.
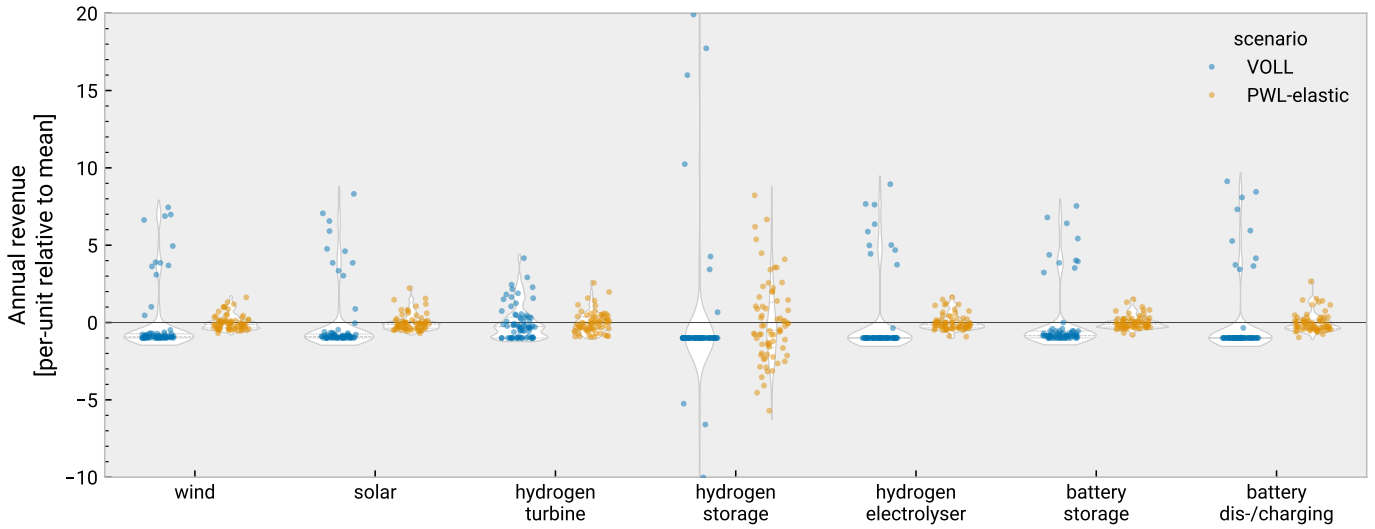
Figure S10: Distribution of annual revenues per technology normalised to the long-term average revenue. Revenues shown are derived from the 70-year LT models with VOLL and PWL-elastic demand. Annual revenues show less year-to-year variation with demand elasticity, similar to average annual baseload prices in Fig. 4. Wind and solar revenues benefit from a natural volume-price hedge: higher availability lowers prices while lower availability raises them, resulting in even tighter revenue clustering.

a) VOLL: perfect foresight
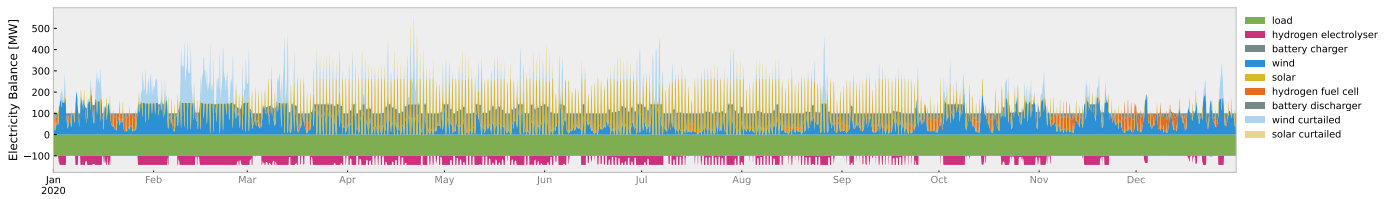
b) VOLL: myopic foresight of 96 hours with overlap of 48 hours and heuristic storage bidding
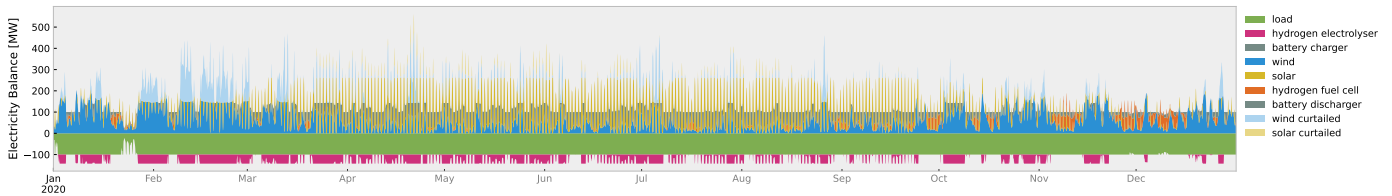
c) PWL-elastic: perfect foresight
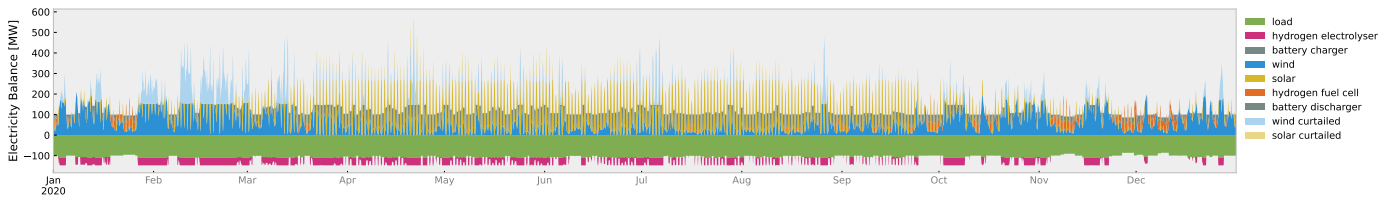
d) PWL-elastic: myopic foresight of 96 hours with overlap of 48 hours and heuristic storage bidding
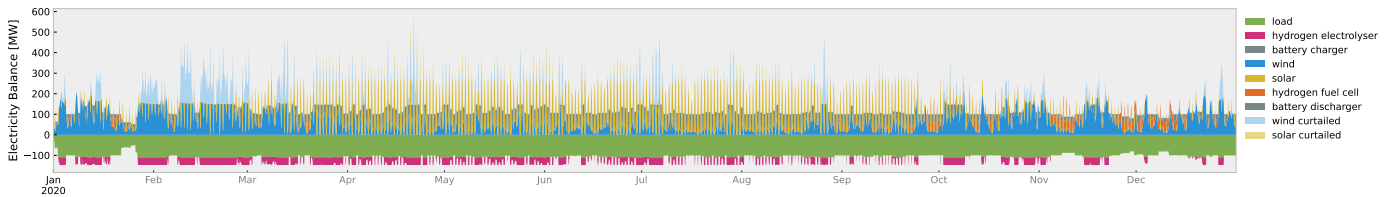
Figure S11: Electricity system balance time series for myopic and perfect operational foresight runs with elastic or inelastic demand for single example year 2020.
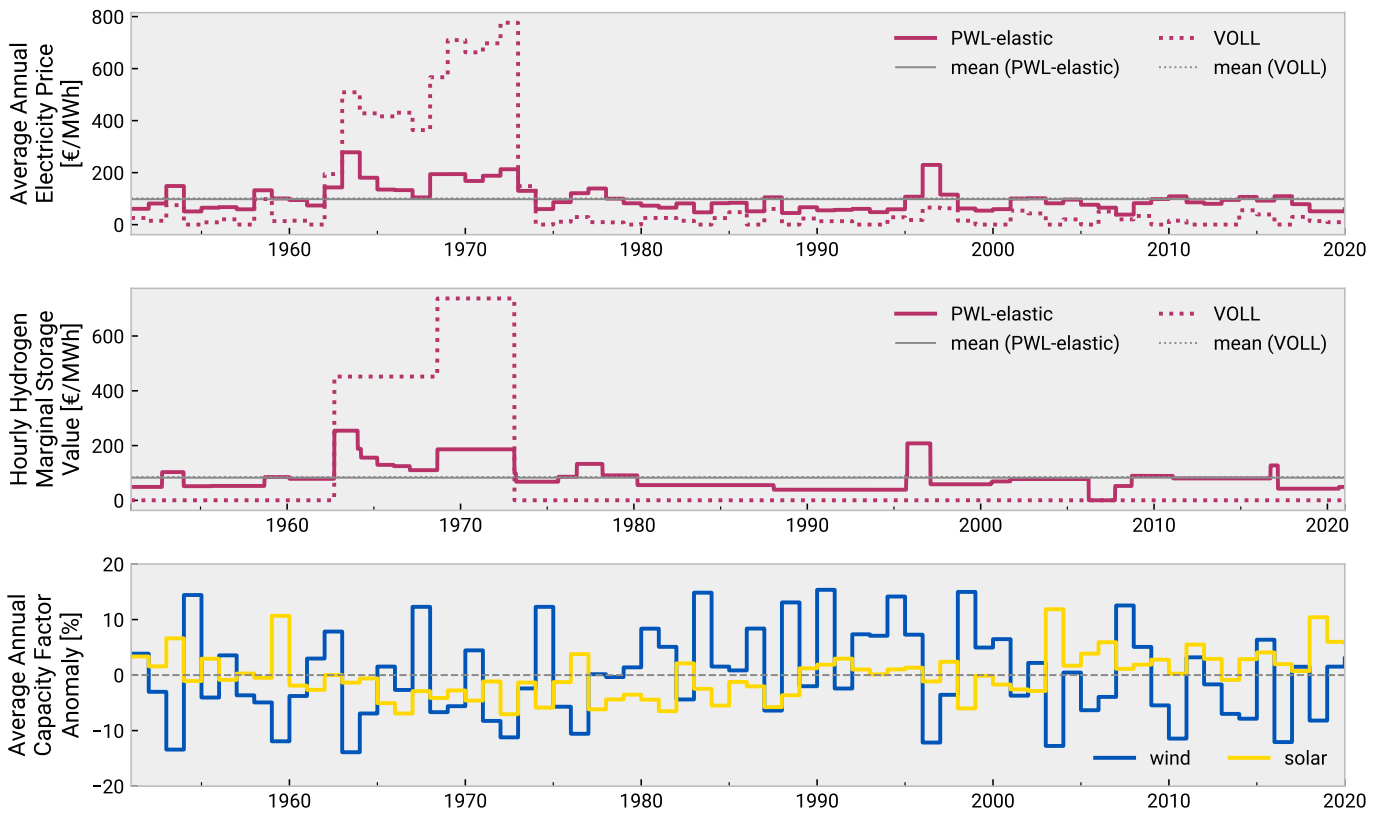
Figure S12: Relation between average annual baseload price, hourly marginal storage values and average annual capacity factor anomaly of wind and solar (i.e. relative deviation from long-term mean) for elastic and inelastic case. High marginal storage values are associated in particular with multi-annual low wind capacity factors, indicating scarcity.

Appendix F. Main figures for different countries

In this section, we replicate the paper's main figures for different countries, namely Spain and the United Kingdom. Figs. S13 and S14 correspond to the price duration curves shown for Germany in Fig. 3. Figs. S15 and S16 replicate the distribution of average annual and monthly baseload prices shown for Germany in Figs. 4 and 5. The comparison of price duration curves and cost recovery factors in different short-term models shown in Figs. S17 and S18 for Spain and the United Kingdom correspond to the comparisons shown for Germany in Figs. 6 and 7. Figs. S19 and S20 show the price and load duration curves for scenarios with cross-elasticity terms. Fig. S21 shows the distribution of annual revenues per technology.
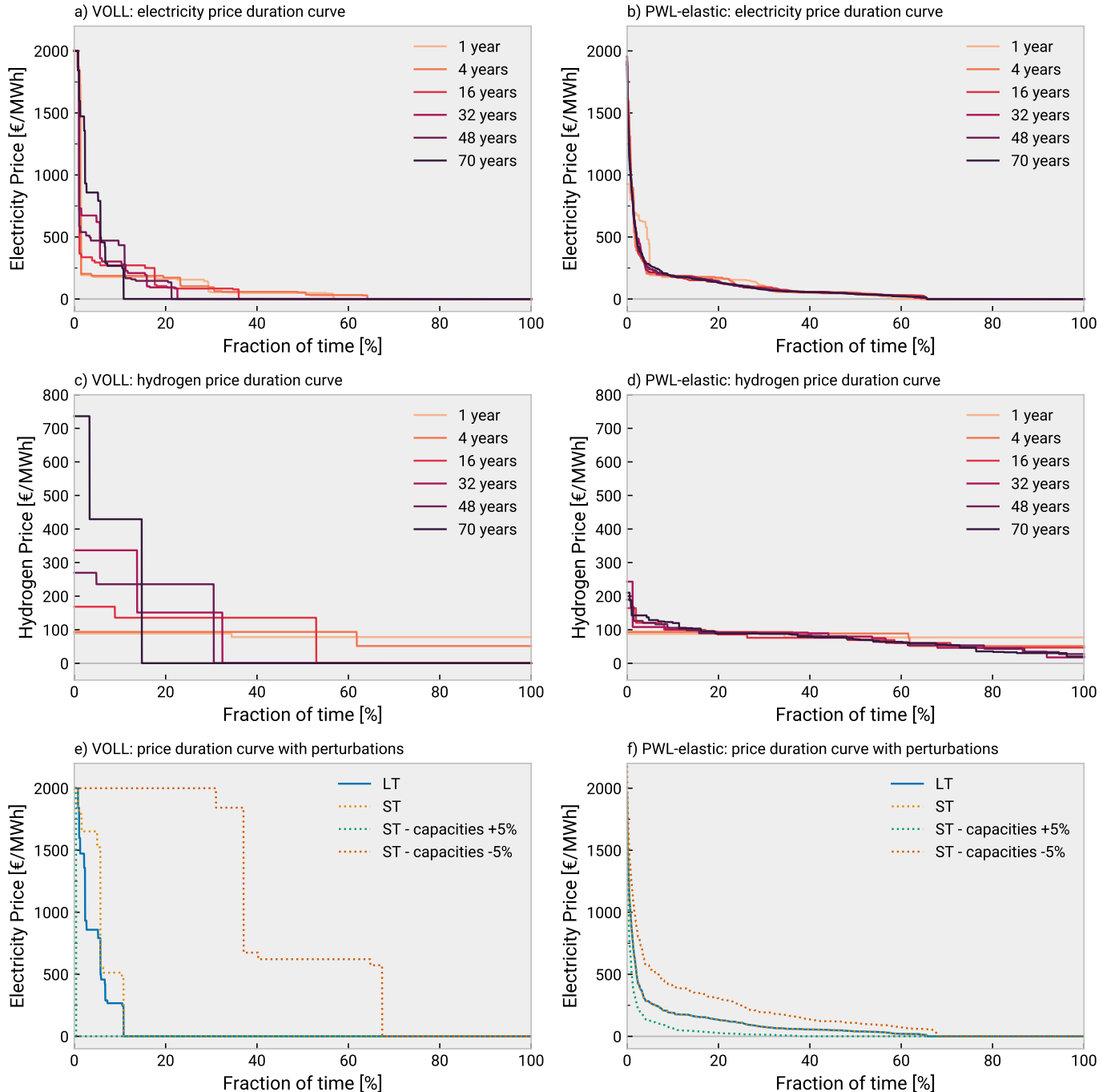
Figure S13: Variant of Fig. 3 for Spain showing electricity and hydrogen price duration curves in long-term and short-term runs with perfect operational foresight.
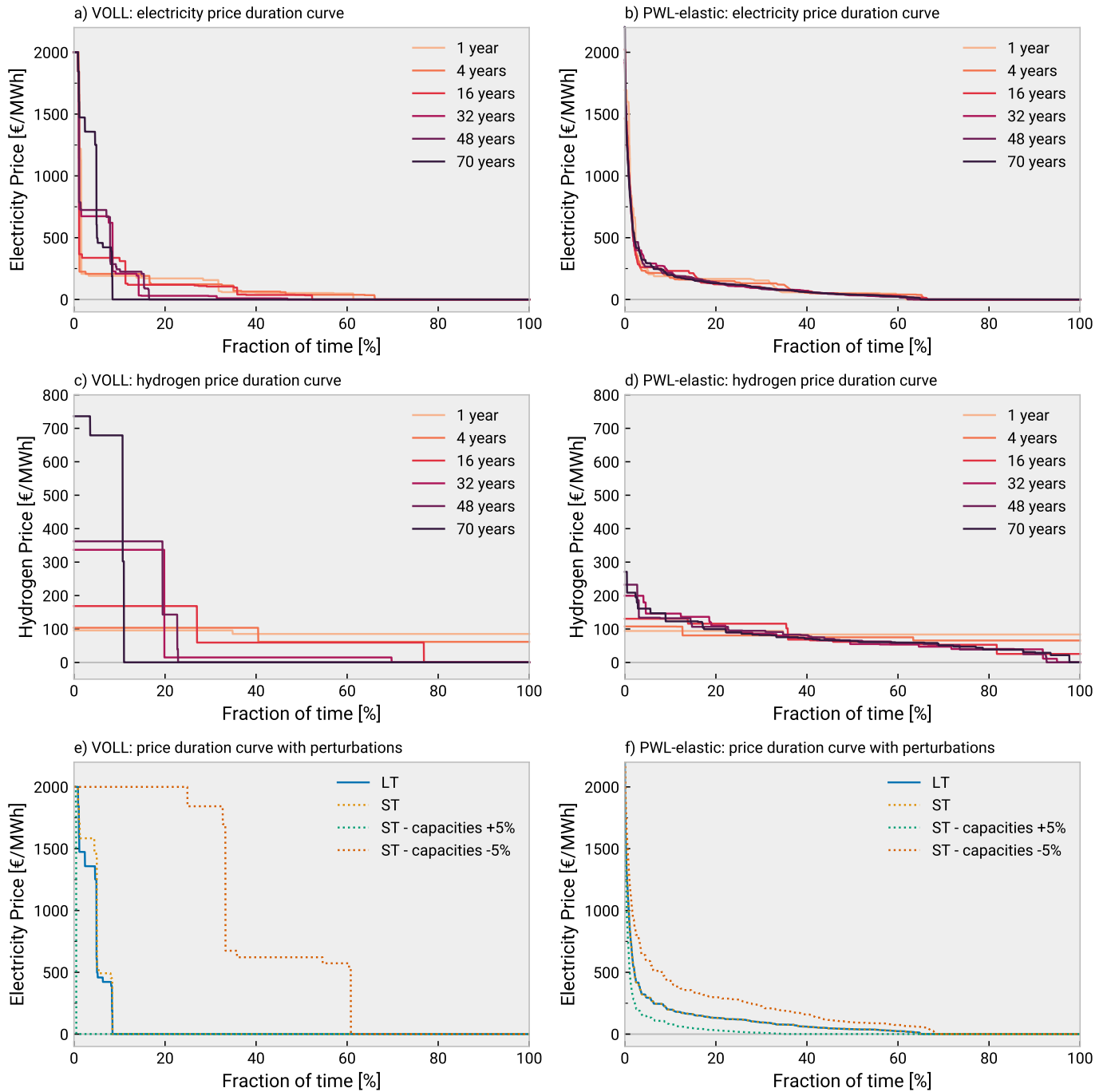
Figure S14: Variant of Fig. 3 for United Kingdom showing electricity and hydrogen price duration curves in long-term and short-term runs with perfect operational foresight.
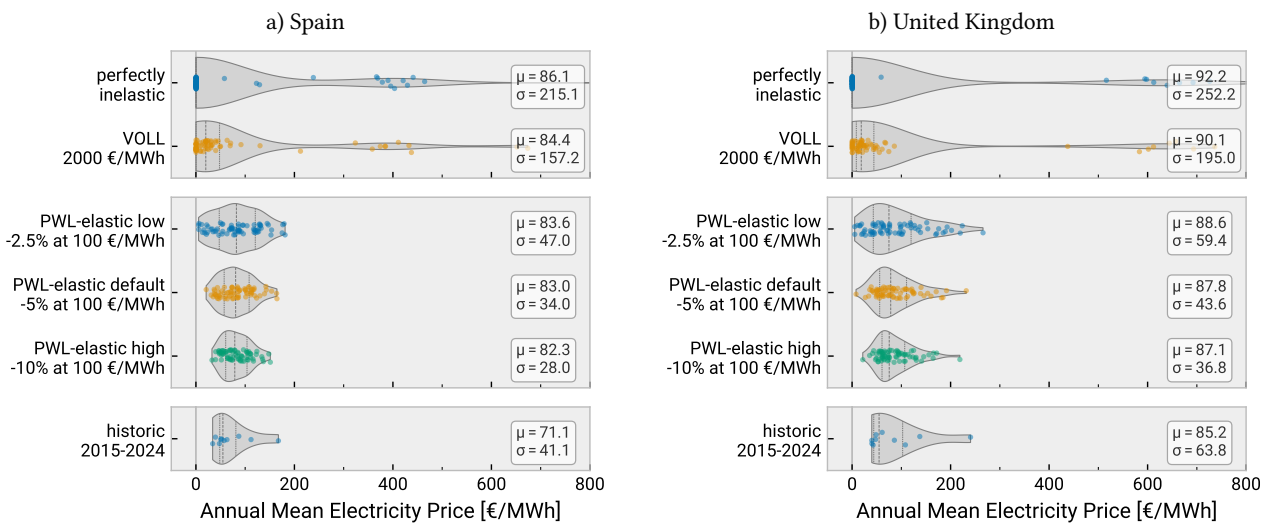
Figure S15: Variant of Fig. 4 for different countries showing distribution of annual average baseload prices.
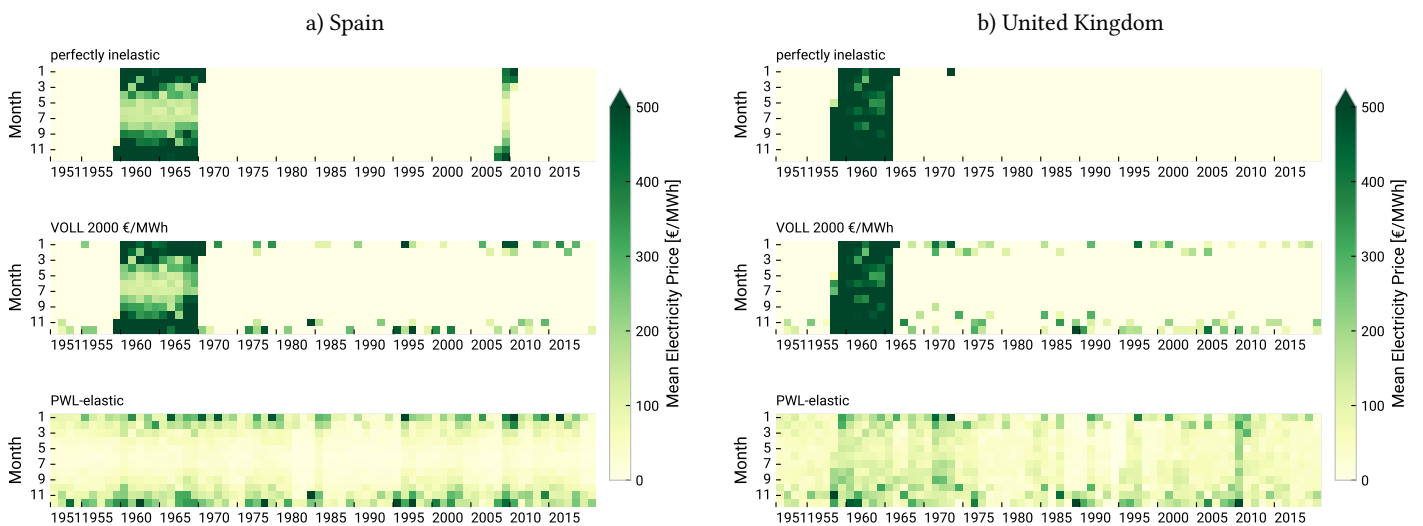
Figure S16: Variant of Fig. 5 for different countries showing heatmap of monthly average baseload prices.

a) Spain

b) United Kingdom
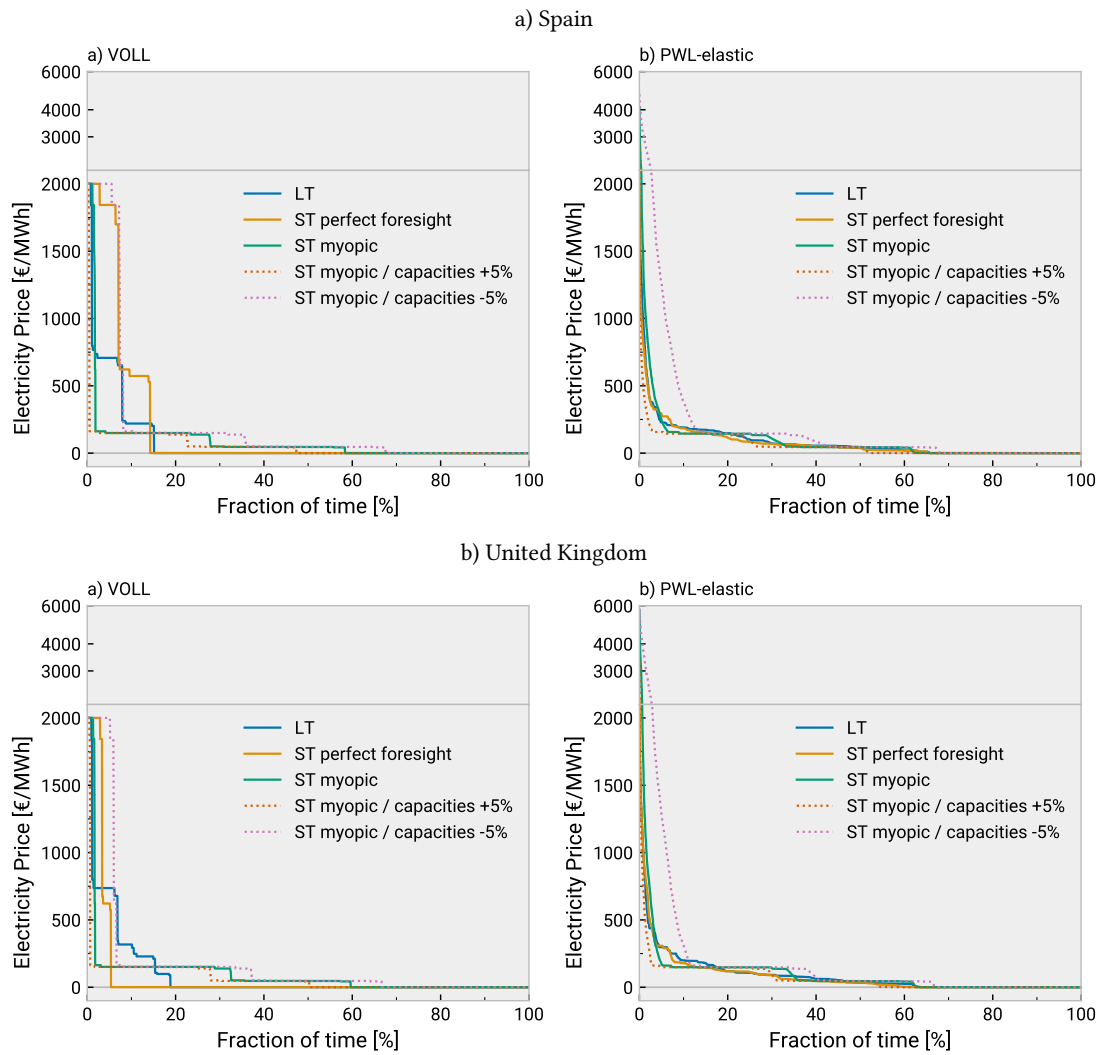
Figure S17: Variant of Fig. 6 for different countries showing price duration curves for runs with myopic foresight.
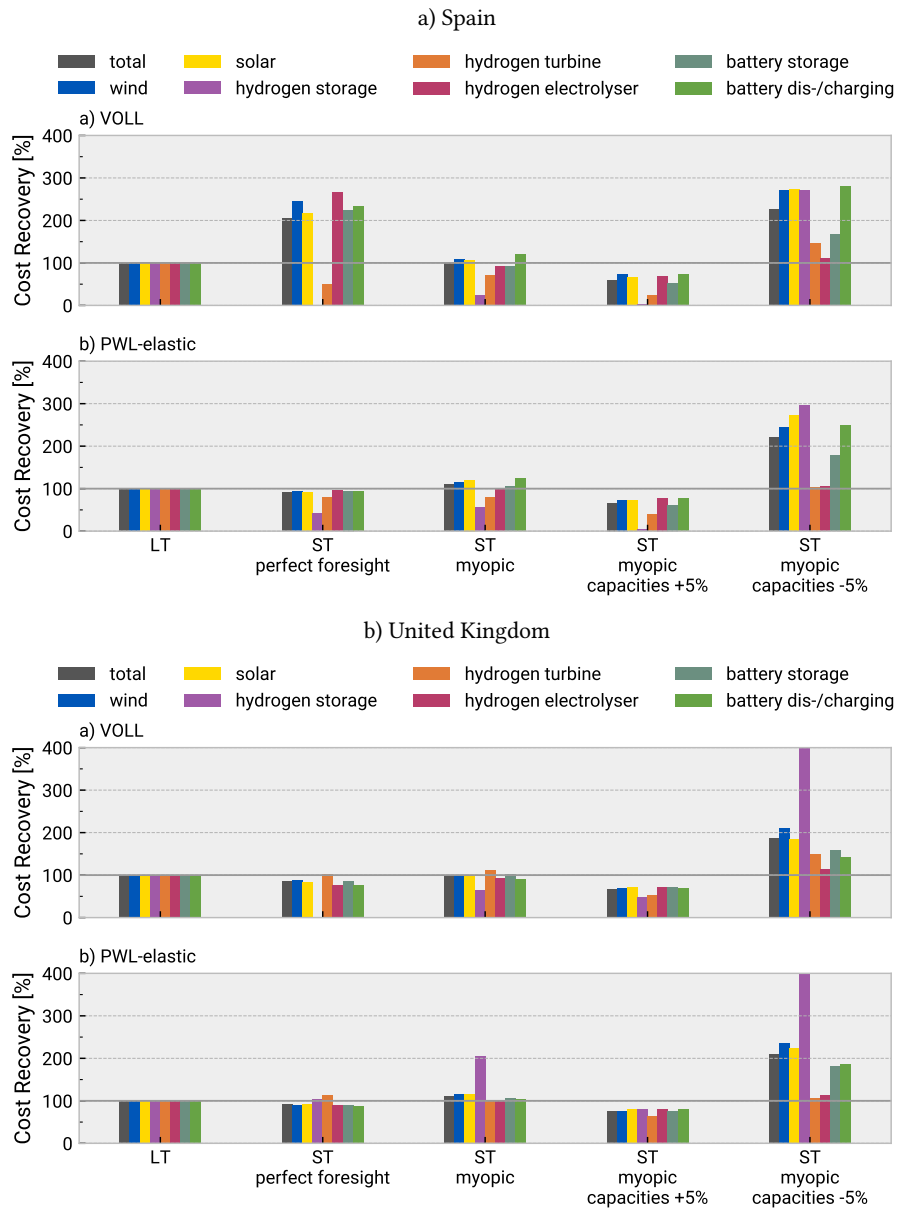
Figure S18: Variant of Fig. 7 for different countries showing cost recovery factors.
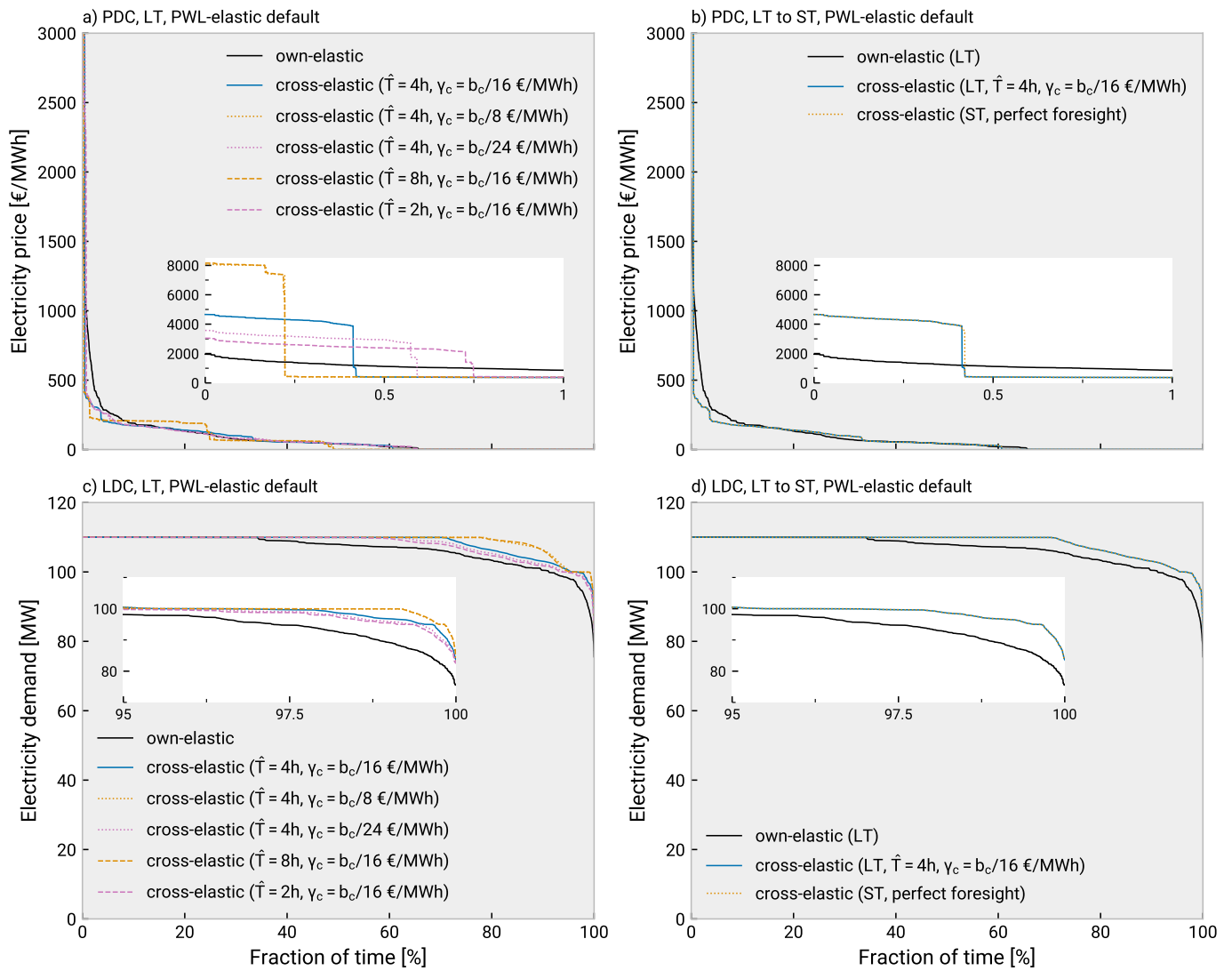
Figure S19: Variant of Fig. S1 for Spain showing price and load duration curves for scenarios with cross-elasticity terms.
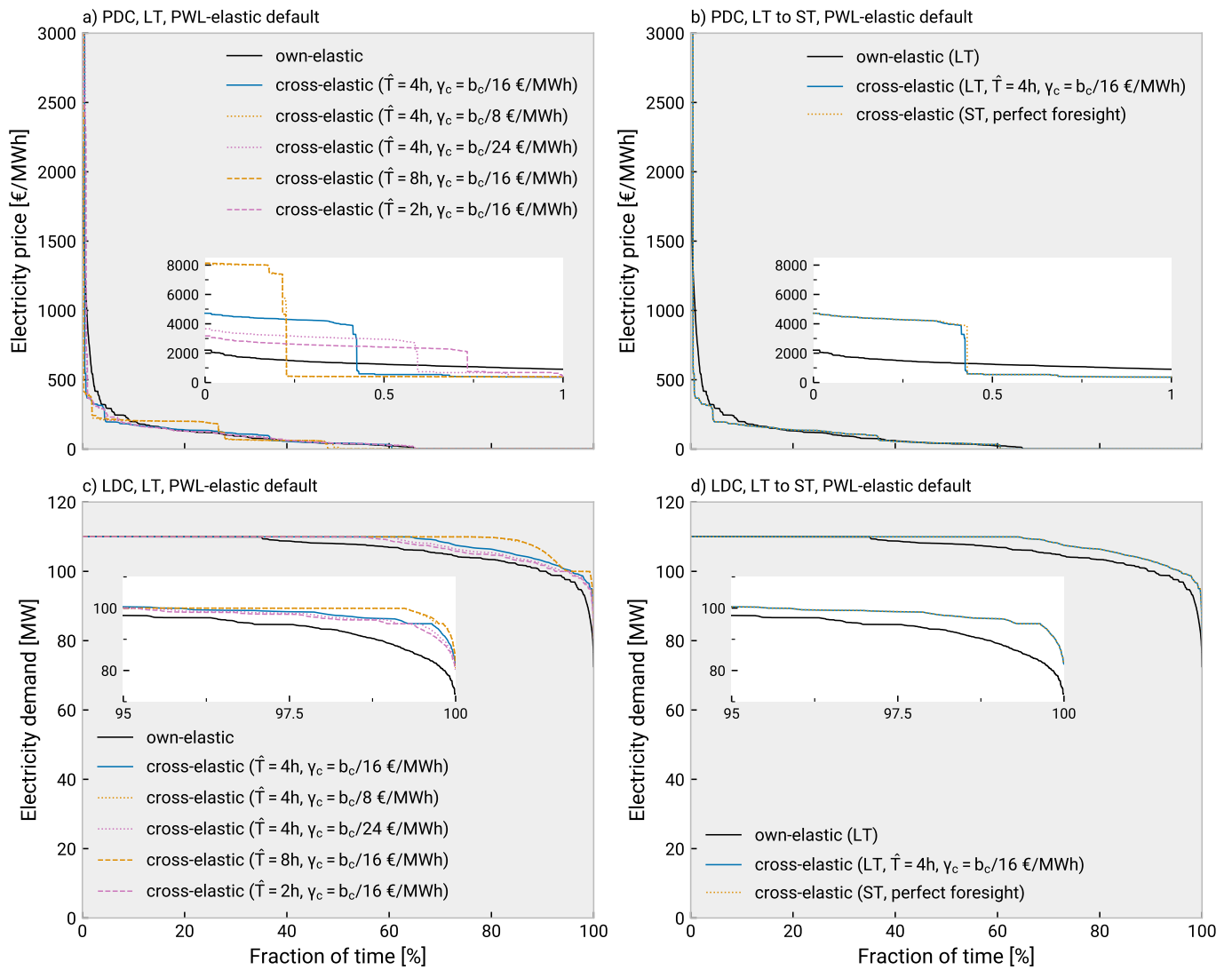
Figure S20: Variant of Fig. S1 for the United Kingdom showing price and load duration curves for scenarios with cross-elasticity terms.
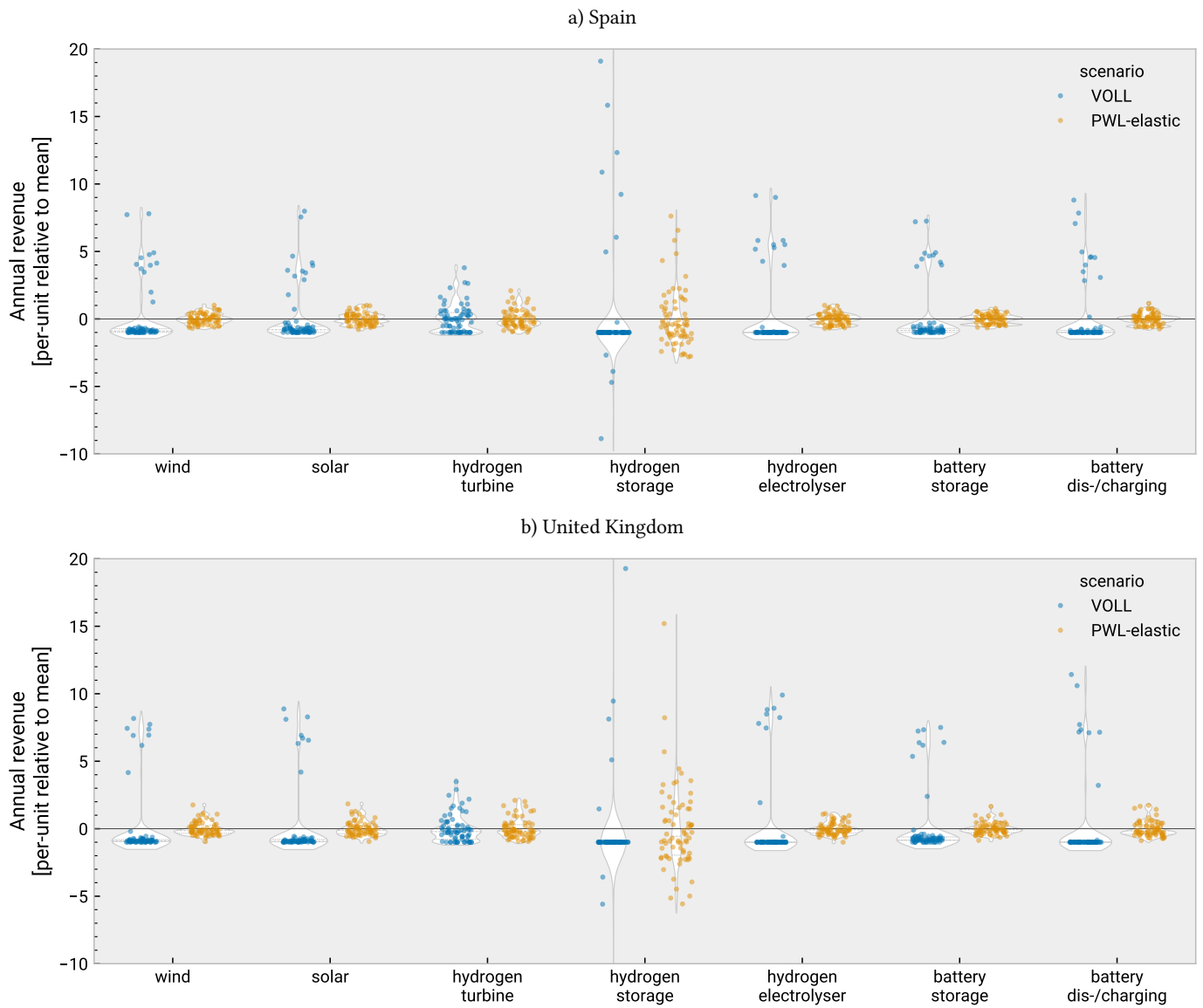
Figure S21: Variant of Fig. S9 showing the distribution of annual revenues per technology for Spain and the United Kingdom.

Appendix G. Additional tables

The tables shown in this section collect a range of metrics for the different cases examined. These metrics include, among other aspects, statistics on prices, load served, system cost, energy mix and capacities built. The tables cover the full 70-year optimisations for Germany (Table S4), Spain (Table S6), and the United Kingdom (Table S8), as well as the model runs where the long-term model was run on 35 different weather years than the 35 weather years the subsequent short-term model was run on for Germany (Table S5), Spain (Table S7), and the United Kingdom (Table S9). Additionally, Table S10 provides statistics for the cases where reserve capacity was forced into the system in Fig. S4

	perfectly inelastic, LT, 70a	VOLL, LT, 70a	PWL-elastic default, LT, 70a	PWL-elastic higher, LT, 70a	PWL-elastic lower, LT, 70a	VOLL, ST, 70a, PF	VOLL, ST, 70a, PF, C+5%	VOLL, ST, 70a, PF, C-5%	PWL-elastic, ST, 70a, PF	PWL-elastic, ST, 70a, PF, C+5%	PWL-elastic, ST, 70a, PF, C-5%
system costs (bn€/period)	6.31	6.15	5.92	5.59	6.16	6.15	6.46	5.84	5.92	6.21	5.62
utility (bn€/period)	–	122.67	468.53	234.03	937.41	122.67	122.71	121.91	468.53	468.72	468.09
welfare (bn€/period)	–	116.52	462.61	228.43	931.25	116.52	116.25	116.07	462.61	462.50	462.47
average system costs (€/MWh)	102.82	100.30	91.02	88.37	93.16	100.30	105.26	95.89	91.02	93.31	89.18
average load served (MW)	100.00	99.95	105.94	103.14	107.77	99.95	99.99	99.34	105.94	108.51	102.73
peak load shedding (MW)	0.00	29.44	33.92	41.53	27.84	29.85	20.67	47.08	33.92	30.04	37.80
primary energy (TWh/period)	72.46	72.43	76.62	73.82	78.56	72.41	70.95	73.03	76.62	78.86	73.78
wind share (%)	45.37	46.88	50.51	50.81	50.31	46.85	43.34	49.68	50.51	49.76	50.93
solar share (%)	54.63	53.12	49.49	49.19	49.69	53.15	56.66	50.32	49.49	50.24	49.07
wind market value (€/MWh)	66.50	66.95	59.69	59.40	59.95	63.01	2.90	393.28	59.69	19.38	126.40
solar market value (€/MWh)	42.20	41.96	41.58	41.51	41.65	39.70	1.84	262.22	41.58	13.11	89.86
wind capacity factor (%)	21.21	21.21	21.21	21.21	21.21	21.21	21.21	21.21	21.21	21.21	21.21
solar capacity factor (%)	11.67	11.67	11.67	11.67	11.67	11.67	11.67	11.67	11.67	11.67	11.67
hydrogen consumed (TWh/period)	9.16	9.19	9.54	8.59	10.26	9.18	7.83	10.03	9.54	10.12	8.78
curtailment (%)	17.11	17.55	12.59	12.33	12.83	17.58	23.08	12.49	12.59	14.33	11.41
wind capacity (MW)	351.56	365.62	371.43	358.19	380.94	365.62	383.91	347.34	371.43	390.00	352.86
solar capacity (MW)	581.65	562.10	548.98	524.76	566.08	562.10	590.21	534.00	548.98	576.43	521.53
electrolyser capacity (MW)	63.00	62.88	55.62	50.41	59.31	62.88	66.03	59.74	55.62	58.40	52.84
fuel cell capacity (MW)	69.54	57.15	46.41	40.15	51.55	57.15	60.01	54.29	46.41	48.73	44.09
battery inverter capacity (MW)	111.54	107.77	107.57	102.79	110.63	107.77	113.16	102.38	107.57	112.95	102.19
battery storage capacity (GWh)	0.81	0.79	0.80	0.76	0.82	0.79	0.83	0.75	0.80	0.84	0.76
hydrogen storage capacity (GWh)	196.68	181.00	112.22	95.02	135.45	181.00	190.05	171.95	112.22	117.83	106.61
mean electricity price (€/MWh)	102.82	101.20	98.02	97.34	98.74	96.37	8.67	570.98	98.02	35.85	199.60
mean hydrogen price (€/MWh)	87.22	85.48	82.81	82.22	83.43	80.71	0.32	568.06	82.81	21.99	183.71
STD electricity price (€/MWh)	1587.53	338.16	166.02	145.49	192.35	318.84	127.95	792.10	166.02	109.00	255.33
STD hydrogen price (€/MWh)	214.16	211.13	49.72	43.10	66.48	192.59	0.00	485.59	49.72	31.32	84.41
mean hydrogen MSV (€/MWh)	87.22	85.48	82.81	82.22	83.43	80.71	0.32	568.06	82.81	21.99	183.71
mean battery MSV (€/MWh)	103.30	101.86	98.87	98.24	99.56	96.97	8.47	577.10	98.87	35.82	202.06
STD hydrogen MSV (€/MWh)	214.16	211.13	49.72	43.10	66.48	192.59	0.00	485.59	49.72	31.32	84.41
STD battery MSV (€/MWh)	1548.41	333.05	161.81	141.67	187.83	313.69	124.84	773.25	161.81	106.56	248.13

Table S4: Metrics for 70-year optimisations for Germany. (PF = perfect foresight; myopic X/Y = myopic foresight with X hours of foresight and Y hours of overlap; VOLL = perfectly inelastic demand up to value of lost load of 2000 €/MWh; PWL-elastic = Piecewise-linear elastic; C±X% = capacity perturbation of ±X%; LT = long-term model; ST = short-term model; STD = Standard Deviation)

<div style="transform: rotate(90deg)">36</div>

	VOLL, LT, 35a	VOLL, ST, 35a-35a, PF	VOLL, ST, 35a-35a, myopic 48/24	VOLL, ST, 35a-35a, myopic 96/48	VOLL, ST, 35a-35a, myopic 96/48, C+5%	VOLL, ST, 35a-35a, myopic 96/48, C-5%	PWL-elastic default, LT, 35a	PWL-elastic default, ST, 35a-35a, PF	PWL-elastic default, ST, 35a-35a, myopic 48/24	PWL-elastic default, ST, 35a-35a, myopic 96/48	PWL-elastic default, ST, 35a-35a, myopic 96/48, C+5%	PWL-elastic default, ST, 35a-35a, myopic 96/48, C-5%
system costs (bn€/period)	3.04	3.04	3.04	3.04	3.19	2.89	2.96	2.96	2.96	2.96	3.11	2.81
utility (bn€/period)	61.34	61.07	61.04	61.06	61.33	60.11	233.02	233.04	232.83	232.87	233.07	232.18
welfare (bn€/period)	58.29	58.03	58.00	58.02	58.14	57.22	230.06	230.08	229.87	229.91	229.96	229.37
average system costs (€/MWh)	99.22	99.65	99.70	99.67	104.18	96.19	91.17	90.81	91.53	91.46	95.03	88.54
average load served (MW)	99.96	99.51	99.47	99.50	99.94	97.94	105.91	106.32	105.47	105.56	106.67	103.60
peak load shedding (MW)	23.96	77.55	88.31	85.60	71.19	93.69	29.90	58.09	71.59	66.89	55.49	83.30
primary energy (TWh/period)	36.67	36.11	36.58	36.61	36.31	35.54	38.20	38.45	37.74	37.82	37.86	37.03
wind share (%)	48.54	48.58	49.43	49.45	48.09	50.10	49.94	51.07	50.51	50.53	49.22	51.51
solar share (%)	51.46	51.42	50.57	50.55	51.91	49.90	50.06	48.93	49.49	49.47	50.78	48.49
wind market value (€/MWh)	61.82	232.08	78.52	79.79	51.07	151.40	60.92	55.51	74.68	74.56	51.55	131.31
solar market value (€/MWh)	41.77	155.51	50.63	51.01	31.47	91.78	41.36	39.36	52.01	50.45	33.56	86.85
wind capacity factor (%)	20.73	21.69	21.69	21.69	21.69	21.69	20.73	21.69	21.69	21.69	21.69	21.69
solar capacity factor (%)	11.78	11.56	11.56	11.56	11.56	11.56	11.78	11.56	11.56	11.56	11.56	11.56
hydrogen consumed (TWh/period)	4.95	4.61	4.59	4.61	4.16	4.50	4.67	4.78	4.28	4.34	4.02	4.26
curtailment (%)	13.20	15.89	14.80	14.74	19.46	12.87	12.34	13.26	14.85	14.67	18.66	12.07
wind capacity (MW)	353.33	353.33	353.33	353.33	370.99	335.66	373.18	373.18	373.18	373.18	391.84	354.52
solar capacity (MW)	547.19	547.19	547.19	547.19	574.55	519.83	549.18	549.18	549.18	549.18	576.64	521.72
electrolyser capacity (MW)	55.60	55.60	55.60	55.60	58.38	52.82	54.67	54.67	54.67	54.67	57.41	51.94
fuel cell capacity (MW)	57.29	57.29	57.29	57.29	60.16	54.43	45.51	45.51	45.51	45.51	47.78	43.23
battery inverter capacity (MW)	107.09	107.09	107.09	107.09	112.44	101.73	108.72	108.72	108.72	108.72	114.16	103.28
battery storage capacity (GWh)	0.79	0.79	0.79	0.79	0.83	0.75	0.81	0.81	0.81	0.81	0.85	0.77
hydrogen storage capacity (GWh)	317.68	317.68	317.68	317.68	333.56	301.79	98.61	98.61	98.61	98.61	103.54	93.67
mean electricity price (€/MWh)	99.93	338.29	136.56	131.32	76.89	235.93	97.80	95.39	131.73	126.23	79.41	236.87
mean hydrogen price (€/MWh)	83.23	348.63	95.00	98.89	68.79	158.86	83.04	75.35	99.25	97.32	67.20	170.19
STD electricity price (€/MWh)	270.09	676.68	356.55	343.06	197.83	532.42	158.09	192.05	368.50	340.12	179.46	651.32
STD hydrogen price (€/MWh)	133.64	476.34	120.83	130.99	56.45	252.28	45.96	69.05	234.24	192.18	78.31	391.13
mean hydrogen MSV (€/MWh)	83.23	348.63	95.00	98.89	68.79	158.86	83.04	75.35	99.25	97.32	67.20	170.19
mean battery MSV (€/MWh)	100.54	342.01	136.15	131.19	77.15	234.52	98.65	95.94	131.92	126.52	79.80	236.19
STD hydrogen MSV (€/MWh)	133.64	476.34	120.83	130.99	56.45	252.28	45.96	69.05	234.24	192.18	78.31	391.13
STD battery MSV (€/MWh)	264.70	664.97	347.52	334.82	193.29	519.41	153.88	187.77	360.79	333.22	176.12	637.72

Table S5: Metrics for 35-year LT plus 35-year ST optimisations for Germany. (PF = perfect foresight; myopic X/Y = myopic foresight with X hours of foresight and Y hours of overlap; VOLL = perfectly inelastic demand up to value of lost load of 2000 €/MWh; PWL-elastic = Piecewise-linear elastic; C±X% = capacity perturbation of ±X%; LT = long-term model; ST = short-term model; STD = Standard Deviation)

	perfectly inelastic, LT, 70a	VOLL, LT, 70a	PWL-elastic default, LT, 70a	PWL-elastic higher, LT, 70a	PWL-elastic lower, LT, 70a	VOLL, ST, 70a, PF	VOLL, ST, 70a, PF, C+5%	VOLL, ST, 70a, PF, C-5%	PWL-elastic, ST, 70a, PF	PWL-elastic, ST, 70a, PF, C+5%	PWL-elastic, ST, 70a, PF, C-5%
system costs (bn€/period)	5.28	5.13	5.03	4.76	5.23	5.13	5.38	4.87	5.03	5.28	4.78
utility (bn€/period)	–	122.67	468.58	234.09	937.46	122.67	122.71	120.80	468.58	468.74	468.20
welfare (bn€/period)	–	117.55	463.55	229.33	932.22	117.55	117.33	115.93	463.55	463.46	463.42
average system costs (€/MWh)	86.08	83.59	76.93	74.56	78.87	83.59	87.72	80.64	76.93	79.06	75.23
average load served (MW)	100.00	99.96	106.51	104.05	108.11	99.96	99.99	98.43	106.51	108.82	103.48
peak load shedding (MW)	0.00	26.93	34.45	41.56	28.65	25.38	15.85	48.31	34.45	30.59	38.30
primary energy (TWh/period)	71.28	71.22	74.95	72.44	76.72	71.22	69.89	69.97	74.95	76.90	72.32
wind share (%)	19.86	20.35	21.22	21.29	21.21	20.35	15.67	22.12	21.22	20.27	21.52
solar share (%)	80.14	79.65	78.78	78.71	78.79	79.65	84.33	77.88	78.78	79.73	78.48
wind market value (€/MWh)	68.20	68.87	62.44	62.14	62.70	107.37	3.33	771.76	62.44	19.54	136.77
solar market value (€/MWh)	30.67	30.92	30.86	30.79	30.91	45.98	2.15	343.25	30.86	10.48	65.50
wind capacity factor (%)	21.86	21.86	21.86	21.86	21.86	21.86	21.86	21.86	21.86	21.86	21.86
solar capacity factor (%)	17.79	17.79	17.79	17.79	17.79	17.79	17.79	17.79	17.79	17.79	17.79
hydrogen consumed (TWh/period)	7.19	7.18	6.76	5.91	7.43	7.18	5.89	6.96	6.76	7.17	6.15
curtailment (%)	18.40	19.20	17.29	17.05	17.46	19.20	24.49	16.43	17.29	19.18	15.99
wind capacity (MW)	155.29	160.57	159.67	154.09	164.04	160.57	168.60	152.54	159.67	167.66	151.69
solar capacity (MW)	609.38	610.12	633.95	610.61	649.88	610.12	640.62	579.61	633.95	665.65	602.26
electrolyser capacity (MW)	43.04	42.59	37.40	32.96	40.92	42.59	44.72	40.46	37.40	39.27	35.53
fuel cell capacity (MW)	60.75	47.83	35.44	29.90	40.19	47.83	50.22	45.43	35.44	37.21	33.66
battery inverter capacity (MW)	163.63	160.49	169.64	163.85	173.27	160.49	168.51	152.47	169.64	178.12	161.16
battery storage capacity (GWh)	1.19	1.16	1.22	1.17	1.24	1.16	1.22	1.10	1.22	1.28	1.16
hydrogen storage capacity (GWh)	157.50	153.86	101.03	85.88	121.12	153.86	161.55	146.17	101.03	106.08	95.98
mean electricity price (€/MWh)	86.08	84.41	82.97	82.35	83.57	123.86	7.69	920.32	82.97	29.18	173.21
mean hydrogen price (€/MWh)	76.02	73.93	72.15	71.66	72.82	122.22	0.32	1000.00	72.15	16.03	167.91
STD electricity price (€/MWh)	1863.44	302.45	155.24	134.53	180.90	406.96	120.37	846.20	155.24	102.50	235.92
STD hydrogen price (€/MWh)	171.61	183.59	33.42	28.53	48.49	292.90	0.00	0.00	33.42	20.18	57.18
mean hydrogen MSV (€/MWh)	76.02	73.93	72.15	71.66	72.82	122.22	0.32	1000.00	72.15	16.03	167.91
mean battery MSV (€/MWh)	86.91	85.32	83.95	83.36	84.54	125.57	7.57	939.07	83.95	29.24	175.91
STD hydrogen MSV (€/MWh)	171.61	183.59	33.42	28.53	48.49	292.90	0.00	0.00	33.42	20.18	57.18
STD battery MSV (€/MWh)	1819.54	298.92	151.94	131.67	177.17	403.39	117.94	815.61	151.94	100.52	230.33

Table S6: Metrics for 70-year optimisations for Spain. (PF = perfect foresight; myopic X/Y = myopic foresight with X hours of foresight and Y hours of overlap; VOLL = perfectly inelastic demand up to value of lost load of 2000 €/MWh; PWL-elastic = Piecewise-linear elastic; C±X% = capacity perturbation of ±X%; LT = long-term model; ST = short-term model; STD = Standard Deviation)

	VOLL, LT, 35a	VOLL, ST, 35a-35a, PF	VOLL, ST, 35a-35a, myopic 48/24	VOLL, ST, 35a-35a, myopic 96/48	VOLL, ST, 35a-35a, myopic 96/48, C+5%	VOLL, ST, 35a-35a, myopic 96/48, C-5%	PWL-elastic default, LT, 35a	PWL-elastic default, ST, 35a-35a, PF	PWL-elastic default, ST, 35a-35a, myopic 48/24	PWL-elastic default, ST, 35a-35a, myopic 96/48	PWL-elastic default, ST, 35a-35a, myopic 96/48, C+5%	PWL-elastic default, ST, 35a-35a, myopic 96/48, C-5%
system costs (bn€/period)	2.58	2.58	2.58	2.58	2.71	2.45	2.53	2.53	2.53	2.53	2.66	2.40
utility (bn€/period)	61.33	61.27	61.24	61.27	61.35	60.63	233.04	233.10	232.97	233.01	233.13	232.46
welfare (bn€/period)	58.75	58.69	58.66	58.69	58.64	58.18	230.51	230.57	230.44	230.48	230.48	230.06
average system costs (€/MWh)	84.15	84.23	84.27	84.24	88.32	80.88	77.44	77.19	77.55	77.52	80.59	75.17
average load served (MW)	99.95	99.85	99.80	99.84	99.97	98.79	106.46	106.80	106.30	106.35	107.39	104.19
peak load shedding (MW)	21.37	59.26	87.81	89.76	63.61	91.42	33.58	34.76	69.07	61.80	44.91	68.80
primary energy (TWh/period)	35.56	35.29	35.41	35.44	34.94	35.12	37.47	37.59	37.19	37.23	37.27	36.27
wind share (%)	18.65	17.76	19.62	19.64	18.24	20.58	21.06	21.05	20.73	20.76	19.63	21.35
solar share (%)	81.35	82.24	80.38	80.36	81.76	79.42	78.94	78.95	79.27	79.24	80.37	78.65
wind market value (€/MWh)	70.09	181.32	76.95	73.38	55.92	166.32	62.75	58.16	71.35	73.47	52.15	148.04
solar market value (€/MWh)	31.42	68.04	36.76	33.92	21.91	84.43	31.08	28.13	38.34	37.40	22.97	83.55
wind capacity factor (%)	21.80	21.93	21.93	21.93	21.93	21.93	21.80	21.93	21.93	21.93	21.93	21.93
solar capacity factor (%)	17.82	17.76	17.76	17.76	17.76	17.76	17.82	17.76	17.76	17.76	17.76	17.76
hydrogen consumed (TWh/period)	3.51	3.30	3.27	3.30	2.75	3.45	3.38	3.39	3.10	3.13	2.82	2.96
curtailment (%)	19.99	20.52	20.27	20.19	25.06	16.76	17.62	17.30	18.18	18.07	21.89	15.99
wind capacity (MW)	149.31	149.31	149.31	149.31	156.78	141.85	158.97	158.97	158.97	158.97	166.92	151.03
solar capacity (MW)	630.50	630.50	630.50	630.50	662.02	598.97	637.65	637.65	637.65	637.65	669.53	605.76
electrolyser capacity (MW)	41.89	41.89	41.89	41.89	43.99	39.80	37.32	37.32	37.32	37.32	39.18	35.45
fuel cell capacity (MW)	48.34	48.34	48.34	48.34	50.75	45.92	36.13	36.13	36.13	36.13	37.94	34.33
battery inverter capacity (MW)	168.33	168.33	168.33	168.33	176.74	159.91	171.02	171.02	171.02	171.02	179.57	162.47
battery storage capacity (GWh)	1.19	1.19	1.19	1.19	1.25	1.13	1.22	1.22	1.22	1.22	1.28	1.16
hydrogen storage capacity (GWh)	141.25	141.25	141.25	141.25	148.31	134.19	104.02	104.02	104.02	104.02	109.22	98.82
mean electricity price (€/MWh)	85.07	175.72	104.68	86.12	52.91	204.42	83.65	75.26	102.14	96.54	56.81	211.47
mean hydrogen price (€/MWh)	74.75	193.73	72.79	75.08	53.36	137.41	72.64	68.86	80.88	82.42	56.90	149.71
STD electricity price (€/MWh)	266.05	496.81	310.38	248.72	134.62	499.34	159.22	138.26	276.88	247.37	104.54	539.77
STD hydrogen price (€/MWh)	144.29	381.63	90.53	99.94	54.64	232.64	31.27	52.44	144.62	126.70	42.51	310.30
mean hydrogen MSV (€/MWh)	74.75	193.73	72.79	75.08	53.36	137.41	72.64	68.86	80.88	82.42	56.90	149.71
mean battery MSV (€/MWh)	85.95	178.21	105.30	87.59	53.78	207.89	84.62	76.21	103.17	97.96	57.73	214.18
STD hydrogen MSV (€/MWh)	144.29	381.63	90.53	99.94	54.64	232.64	31.27	52.44	144.62	126.70	42.51	310.30
STD battery MSV (€/MWh)	262.33	492.92	305.23	247.56	132.94	496.70	155.85	135.76	273.00	245.24	102.95	534.58

Table S7: Metrics for 35-year LT plus 35-year ST optimisations for Spain. (PF = perfect foresight; myopic X/Y = myopic foresight with X hours of foresight and Y hours of overlap; VOLL = perfectly inelastic demand up to value of lost load of 2000 €/MWh; PWL-elastic = Piecewise-linear elastic; C±X% = capacity perturbation of ±X%; LT = long-term model; ST = short-term model; STD = Standard Deviation)

	perfectly inelastic, LT, 70a	VOLL, LT, 70a	PWL-elastic default, LT, 70a	PWL-elastic higher, LT, 70a	PWL-elastic lower, LT, 70a	VOLL, ST, 70a, PF	VOLL, ST, 70a, PF, C+5%	VOLL, ST, 70a, PF, C-5%	PWL-elastic, ST, 70a, PF	PWL-elastic, ST, 70a, PF, C+5%	PWL-elastic, ST, 70a, PF, C-5%
system costs (bn€/period)	5.66	5.47	5.30	5.00	5.52	5.47	5.74	5.20	5.30	5.56	5.04
utility (bn€/period)	–	122.66	468.55	234.06	937.43	122.66	122.70	121.52	468.55	468.72	468.16
welfare (bn€/period)	–	117.19	463.25	229.06	931.91	117.19	116.96	116.33	463.25	463.16	463.13
average system costs (€/MWh)	92.19	89.16	81.21	78.58	83.27	89.16	93.57	85.50	81.21	83.40	79.40
average load served (MW)	100.00	99.95	106.34	103.76	108.01	99.95	99.98	99.02	106.34	108.72	103.33
peak load shedding (MW)	0.00	29.62	37.56	45.45	31.15	26.41	21.56	44.13	37.56	33.87	41.26
primary energy (TWh/period)	74.87	74.16	78.42	75.61	80.26	74.16	72.67	74.13	78.42	80.52	75.64
wind share (%)	67.43	66.27	67.01	66.94	66.87	66.27	63.88	67.92	67.01	66.29	67.48
solar share (%)	32.57	33.73	32.99	33.06	33.13	33.73	36.12	32.08	32.99	33.71	32.52
wind market value (€/MWh)	46.82	47.18	44.11	43.86	44.32	53.15	2.32	477.35	44.11	13.55	94.93
solar market value (€/MWh)	44.12	44.15	44.16	44.15	44.16	50.49	1.89	500.91	44.16	12.73	98.07
wind capacity factor (%)	29.11	29.11	29.11	29.11	29.11	29.11	29.11	29.11	29.11	29.11	29.11
solar capacity factor (%)	10.63	10.63	10.63	10.63	10.63	10.63	10.63	10.63	10.63	10.63	10.63
hydrogen consumed (TWh/period)	11.78	11.13	11.29	10.18	12.02	11.13	9.78	11.55	11.29	11.88	10.47
curtailment (%)	18.85	19.05	15.17	14.81	15.43	19.05	24.46	14.83	15.17	17.04	13.86
wind capacity (MW)	379.67	372.40	372.19	356.49	381.94	372.40	391.02	353.78	372.19	390.80	353.58
solar capacity (MW)	374.61	384.54	397.80	384.23	408.89	384.54	403.77	365.31	397.80	417.69	377.91
electrolyser capacity (MW)	72.16	68.00	61.97	56.08	65.65	68.00	71.40	64.60	61.97	65.07	58.87
fuel cell capacity (MW)	77.67	61.67	49.91	42.98	55.63	61.67	64.76	58.59	49.91	52.40	47.41
battery inverter capacity (MW)	62.01	67.63	70.86	69.19	72.53	67.63	71.01	64.25	70.86	74.40	67.31
battery storage capacity (GWh)	0.48	0.53	0.56	0.55	0.57	0.53	0.56	0.51	0.56	0.59	0.53
hydrogen storage capacity (GWh)	164.12	155.33	95.58	80.36	113.57	155.33	163.10	147.56	95.58	100.36	90.80
mean electricity price (€/MWh)	92.19	90.14	87.84	87.12	88.60	100.21	9.61	820.48	87.84	31.83	179.66
mean hydrogen price (€/MWh)	77.35	75.63	73.95	73.38	74.51	86.82	0.32	879.28	73.95	18.14	167.44
STD electricity price (€/MWh)	1315.41	338.78	165.33	142.35	194.57	370.80	134.94	841.26	165.33	113.37	246.63
STD hydrogen price (€/MWh)	219.81	215.94	42.29	37.18	58.75	246.69	0.00	308.17	42.29	26.39	72.39
mean hydrogen MSV (€/MWh)	77.35	75.63	73.95	73.38	74.51	86.82	0.32	879.28	73.95	18.14	167.44
mean battery MSV (€/MWh)	92.51	90.82	88.77	88.11	89.46	101.08	9.38	832.24	88.77	31.86	182.14
STD hydrogen MSV (€/MWh)	219.81	215.94	42.29	37.18	58.75	246.69	0.00	308.17	42.29	26.39	72.39
STD battery MSV (€/MWh)	1283.92	334.27	161.34	138.89	190.07	366.33	131.47	815.92	161.34	110.79	240.44

Table S8: Metrics for 70-year optimisations for the United Kingdom. (PF = perfect foresight; myopic X/Y = myopic foresight with X hours of foresight and Y hours of overlap; VOLL = perfectly inelastic demand up to value of lost load of 2000 €/MWh; PWL-elastic = Piecewise-linear elastic; C±X% = capacity perturbation of ±X%; LT = long-term model; ST = short-term model; STD = Standard Deviation)

	VOLL, LT, 35a	VOLL, ST, 35a-35a, PF	VOLL, ST, 35a-35a, myopic 48/24	VOLL, ST, 35a-35a, myopic 96/48	VOLL, ST, 35a-35a, myopic 96/48, C+5%	VOLL, ST, 35a-35a, myopic 96/48, C-5%	PWL-elastic default, LT, 35a	PWL-elastic default, ST, 35a-35a, PF	PWL-elastic default, ST, 35a-35a, myopic 48/24	PWL-elastic default, ST, 35a-35a, myopic 96/48	PWL-elastic default, ST, 35a-35a, myopic 96/48, C+5%	PWL-elastic default, ST, 35a-35a, myopic 96/48, C-5%
system costs (bn€/period)	2.73	2.73	2.73	2.73	2.86	2.59	2.66	2.66	2.66	2.66	2.79	2.52
utility (bn€/period)	61.33	61.27	61.25	61.27	61.35	60.64	233.03	233.07	232.89	232.92	233.10	232.27
welfare (bn€/period)	58.60	58.54	58.53	58.54	58.48	58.05	230.37	230.41	230.24	230.26	230.31	229.74
average system costs (€/MWh)	88.92	89.01	89.03	89.01	93.32	85.45	81.47	81.19	81.71	81.68	85.05	79.08
average load served (MW)	99.95	99.84	99.81	99.84	99.97	98.81	106.35	106.70	106.02	106.06	106.93	104.07
peak load shedding (MW)	30.10	48.61	85.67	84.69	68.12	99.11	33.84	38.18	91.05	81.65	51.10	87.39
primary energy (TWh/period)	37.16	36.99	37.26	37.27	36.65	36.98	39.09	39.31	38.79	38.83	38.69	37.93
wind share (%)	65.97	66.25	66.55	66.53	64.42	67.90	66.76	67.37	66.95	66.97	65.27	67.85
solar share (%)	34.03	33.75	33.45	33.47	35.58	32.10	33.24	32.63	33.05	33.03	34.73	32.15
wind market value (€/MWh)	46.87	40.88	47.45	46.25	35.15	92.07	44.88	39.32	51.69	51.86	36.95	101.88
solar market value (€/MWh)	44.01	37.10	45.36	44.26	32.49	82.14	44.01	40.55	52.01	51.19	36.29	99.87
wind capacity factor (%)	28.78	29.44	29.44	29.44	29.44	29.44	28.78	29.44	29.44	29.44	29.44	29.44
solar capacity factor (%)	10.70	10.56	10.56	10.56	10.56	10.56	10.70	10.56	10.56	10.56	10.56	10.56
hydrogen consumed (TWh/period)	5.63	5.51	5.50	5.51	4.90	5.67	5.54	5.63	5.25	5.27	4.89	5.10
curtailment (%)	17.84	19.27	18.68	18.65	23.81	15.05	15.39	15.99	17.10	17.02	21.26	14.68
wind capacity (MW)	368.54	368.54	368.54	368.54	386.96	350.11	375.61	375.61	375.61	375.61	394.39	356.83
solar capacity (MW)	386.40	386.40	386.40	386.40	405.72	367.08	396.95	396.95	396.95	396.95	416.80	377.11
electrolyser capacity (MW)	66.79	66.79	66.79	66.79	70.13	63.45	60.94	60.94	60.94	60.94	63.98	57.89
fuel cell capacity (MW)	61.38	61.38	61.38	61.38	64.45	58.31	49.10	49.10	49.10	49.10	51.56	46.65
battery inverter capacity (MW)	68.15	68.15	68.15	68.15	71.56	64.74	71.53	71.53	71.53	71.53	75.11	67.96
battery storage capacity (GWh)	0.53	0.53	0.53	0.53	0.56	0.51	0.57	0.57	0.57	0.57	0.60	0.54
hydrogen storage capacity (GWh)	157.72	157.72	157.72	157.72	165.61	149.84	87.49	87.49	87.49	87.49	91.86	83.12
mean electricity price (€/MWh)	89.92	78.82	98.93	91.86	63.82	181.91	88.35	82.02	110.15	107.83	70.17	223.67
mean hydrogen price (€/MWh)	75.57	61.81	72.48	72.72	55.75	123.70	74.45	65.41	88.52	86.12	60.45	163.10
STD electricity price (€/MWh)	267.78	363.86	271.10	250.11	162.37	458.81	167.48	175.47	339.43	319.51	150.22	623.97
STD hydrogen price (€/MWh)	135.66	240.18	64.77	75.24	41.62	205.31	47.23	50.88	235.75	180.71	50.86	394.59
mean hydrogen MSV (€/MWh)	75.57	61.81	72.48	72.72	55.75	123.70	74.45	65.41	88.52	86.12	60.45	163.10
mean battery MSV (€/MWh)	90.61	78.90	98.99	92.13	64.26	181.00	89.28	82.75	110.87	108.50	70.97	224.46
STD hydrogen MSV (€/MWh)	135.66	240.18	64.77	75.24	41.62	205.31	47.23	50.88	235.75	180.71	50.86	394.59
STD battery MSV (€/MWh)	262.56	357.87	263.76	243.55	158.53	447.10	163.49	171.30	333.21	313.40	147.81	613.99

Table S9: Metrics for 35-year LT plus 35-year ST optimisations for the United Kingdom. (PF = perfect foresight; myopic X/Y = myopic foresight with X hours of foresight and Y hours of overlap; VOLL = perfectly inelastic demand up to value of lost load of 2000 €/MWh; PWL-elastic = Piecewise-linear elastic; C±X% = capacity perturbation of ±X%; LT = long-term model; ST = short-term model; STD = Standard Deviation)

	VOLL, 0 MW	VOLL, 10 MW	VOLL, 30 MW	VOLL, 50 MW	VOLL, 70 MW	VOLL, 90 MW	linear-elastic, 0 MW	linear-elastic, 10 MW	linear-elastic, 30 MW	linear-elastic, 50 MW	linear-elastic, 70 MW	linear-elastic, 90 MW
system costs (bn€/period)	1.71	1.71	1.71	1.71	1.75	1.82	1.47	1.47	1.47	1.55	1.62	1.68
utility (bn€/period)	35.05	35.05	35.05	35.05	35.06	35.06	17.42	17.42	17.42	17.47	17.47	17.47
welfare (bn€/period)	33.34	33.34	33.34	33.34	33.31	33.25	15.96	15.96	15.96	15.92	15.85	15.79
average system costs (€/MWh)	97.54	97.54	97.54	97.54	99.76	103.61	88.00	88.00	88.00	92.24	96.29	100.32
average load served (MW)	99.97	99.97	99.97	99.97	100.00	100.00	95.19	95.19	95.19	95.66	95.71	95.71
peak load shedding (MW)	17.57	17.26	18.21	20.55	0.00	0.00	37.65	37.65	37.65	19.50	14.96	14.96
primary energy (TWh/period)	20.84	20.84	20.84	20.84	21.07	21.07	19.37	19.37	19.37	19.73	19.77	19.77
wind share (%)	49.55	49.55	49.55	49.55	51.02	51.02	50.37	50.37	50.37	50.98	51.04	51.04
solar share (%)	50.45	50.45	50.45	50.45	48.98	48.98	49.63	49.63	49.63	49.02	48.96	48.96
wind market value (€/MWh)	63.14	63.14	63.14	63.14	60.83	60.83	61.86	61.86	61.86	60.33	60.23	60.22
solar market value (€/MWh)	40.71	40.71	40.71	40.71	40.56	40.56	40.70	40.70	40.70	40.49	40.47	40.47
wind capacity factor (%)	20.74	20.74	20.74	20.74	20.74	20.74	20.74	20.74	20.74	20.74	20.74	20.74
solar capacity factor (%)	12.04	12.04	12.04	12.04	12.04	12.04	12.04	12.04	12.04	12.04	12.04	12.04
hydrogen consumed (TWh/period)	2.74	2.74	2.74	2.74	2.96	2.96	2.18	2.18	2.18	2.44	2.46	2.46
curtailment (%)	13.81	13.81	13.81	13.81	12.12	12.12	12.96	12.96	12.96	11.65	11.55	11.55
wind capacity (MW)	364.89	364.89	364.89	364.89	366.13	366.12	337.88	337.88	337.88	339.72	340.09	340.09
solar capacity (MW)	516.67	516.67	516.67	516.67	505.41	505.40	472.46	472.46	472.46	472.88	472.84	472.84
electrolyser capacity (MW)	57.53	57.53	57.53	57.53	60.95	60.94	44.43	44.43	44.43	51.69	52.34	52.35
fuel cell capacity (MW)	58.10	58.10	58.10	58.10	70.00	90.00	32.00	32.00	32.00	50.00	70.00	90.00
battery inverter capacity (MW)	104.84	104.84	104.84	104.84	100.11	100.11	95.95	95.95	95.95	94.40	94.19	94.19
battery storage capacity (GWh)	0.79	0.79	0.79	0.79	0.73	0.73	0.72	0.72	0.72	0.69	0.69	0.69
hydrogen storage capacity (GWh)	131.02	131.02	131.02	131.02	195.40	195.45	80.84	80.84	80.84	90.99	90.65	90.66
mean electricity price (€/MWh)	98.21	98.21	98.21	98.21	86.32	86.28	96.12	96.12	96.12	86.85	85.76	85.76
mean hydrogen price (€/MWh)	84.65	84.65	84.65	84.65	89.46	89.48	80.63	80.63	80.63	88.31	88.89	88.89
STD electricity price (€/MWh)	238.02	238.02	238.02	238.02	151.01	150.86	124.29	124.29	124.29	85.22	82.35	82.35
STD hydrogen price (€/MWh)	98.77	98.77	98.77	98.77	103.89	103.89	28.14	28.14	28.14	28.46	27.69	27.70
mean hydrogen MSV (€/MWh)	84.65	84.65	84.65	84.65	89.46	89.48	80.63	80.63	80.63	88.31	88.89	88.89
mean battery MSV (€/MWh)	98.86	98.86	98.86	98.86	87.08	87.01	97.09	97.09	97.09	87.87	86.58	86.57
STD hydrogen MSV (€/MWh)	98.77	98.77	98.77	98.77	103.89	103.89	28.14	28.14	28.14	28.46	27.69	27.70
STD battery MSV (€/MWh)	232.31	232.31	232.31	232.31	147.82	147.62	120.70	120.70	120.70	82.29	79.15	79.14

Table S10: Metrics for 20-year LT optimisations (2001-2020) for Germany with forced reserve capacity (hydrogen turbine). VOLL with 2000 €/MWh. Linear-elastic demand with $a = 2000$ and $b = 10$.